Manufacturing Engineering and Technology

Eighth Edition

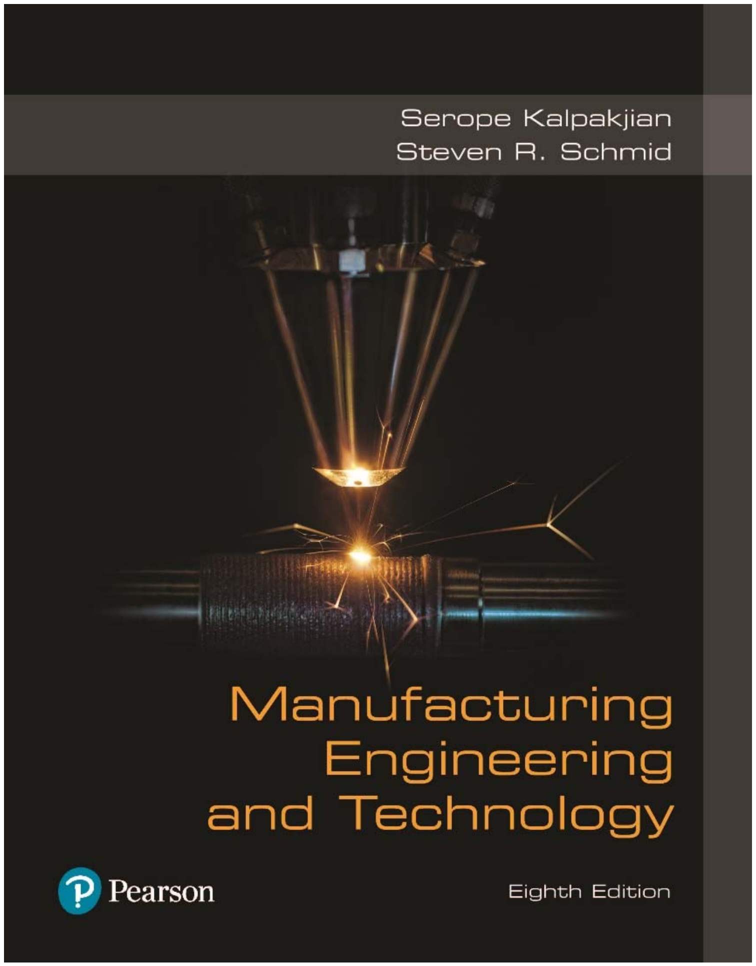

Chapter 1-2

The Structure of Metals

TABLE I.1 Approximate Number of Parts in Products

TABLE I.1

Approximate Number of Parts in Products	
Common pencil	4
Rotary lawn mower	300
Grand piano	12,000
Automobile	15,000
Boeing 747–400	6,000,000

FIGURE I.1 Model 8430 John Deere tractor, with detailed illustration of its diesel engine, showing the variety of materials and processes incorporated. ***Source:*** **Courtesy of John Deere Company.**

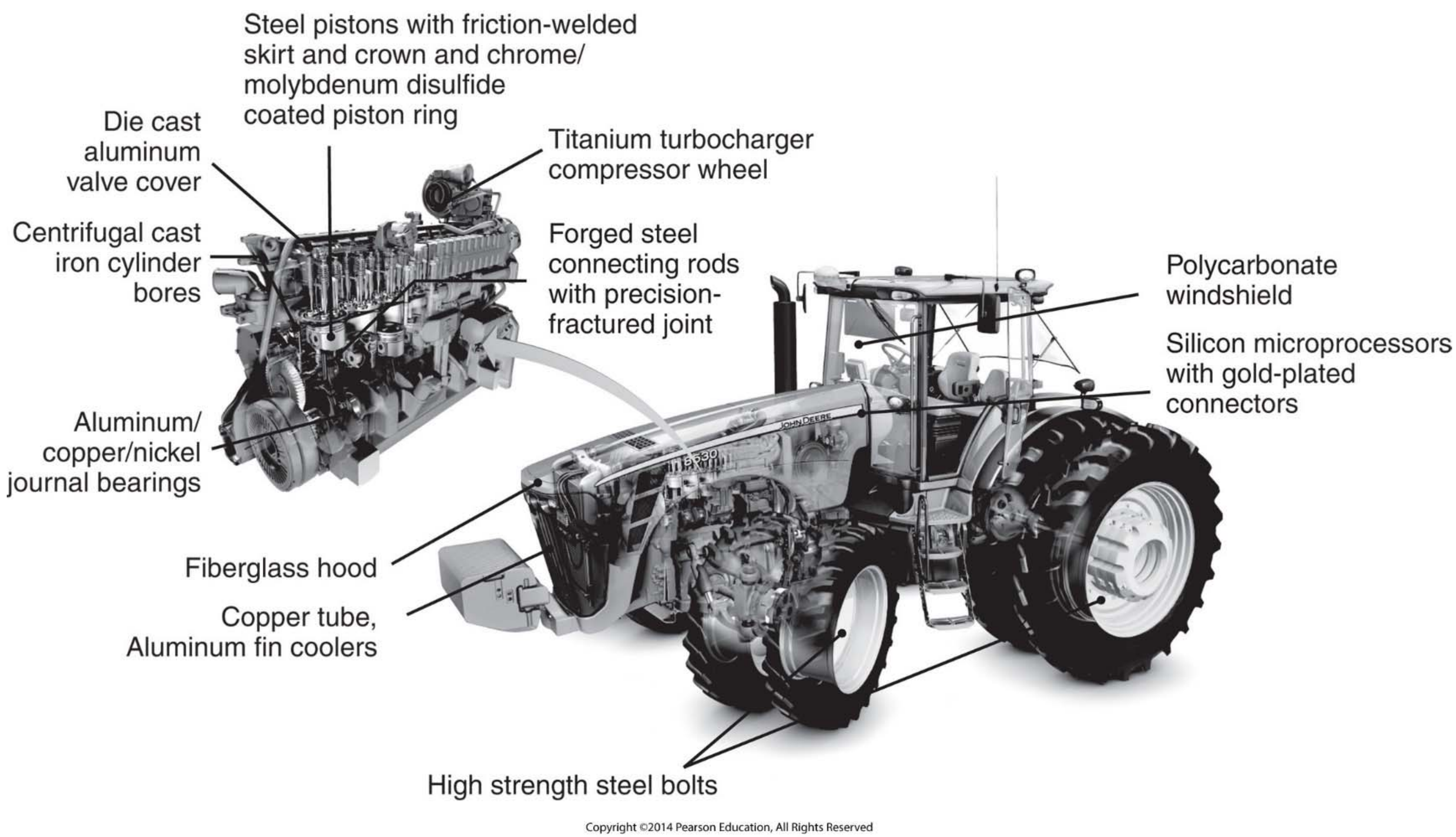

FIGURE I.2 (a) Chart showing various steps involved in *traditional design* and manufacture of a product. Depending on the complexity of the product and the type of materials used, the time span between the original concept and the marketing of the product may range from a few months to several years. (b) Chart showing general product flow in *concurrent engineering*, from market analysis to marketing the product.
Source: After S. Pugh.

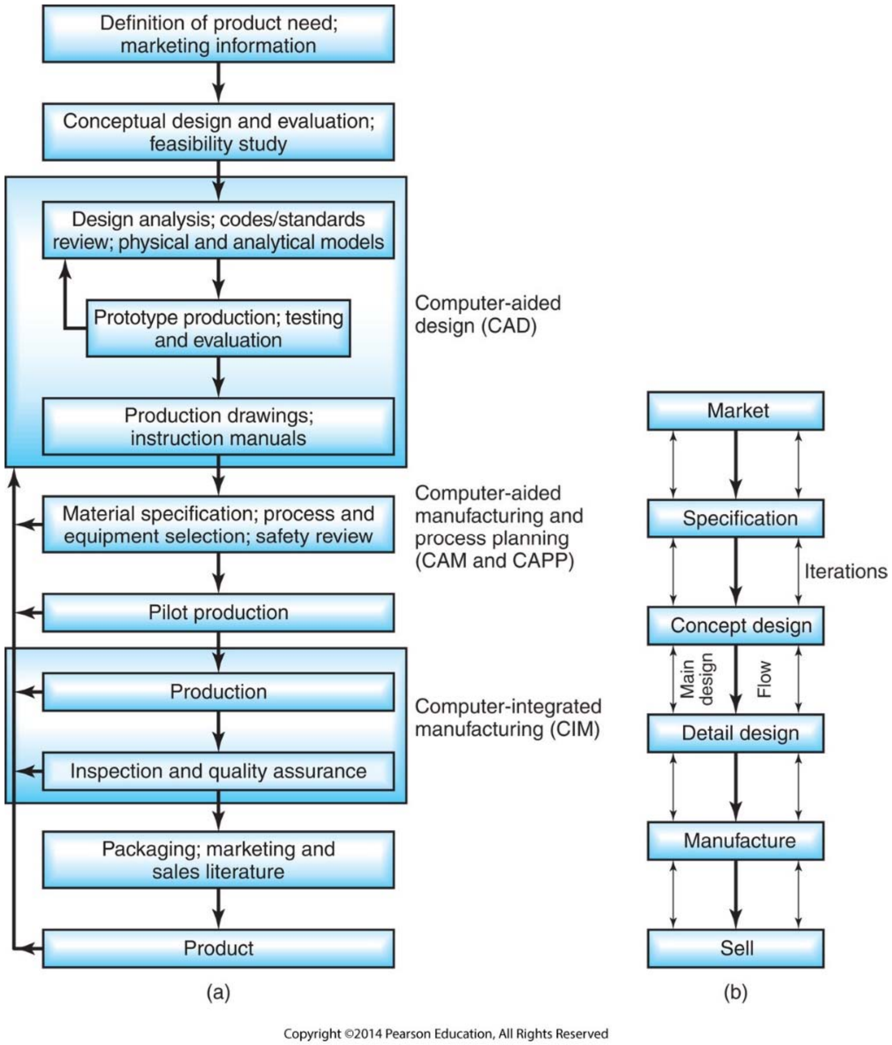

FIGURE I.3 Redesign of parts to facilitate assembly. ***Source:*** **After G. Boothroyd and P. Dewhurst.**

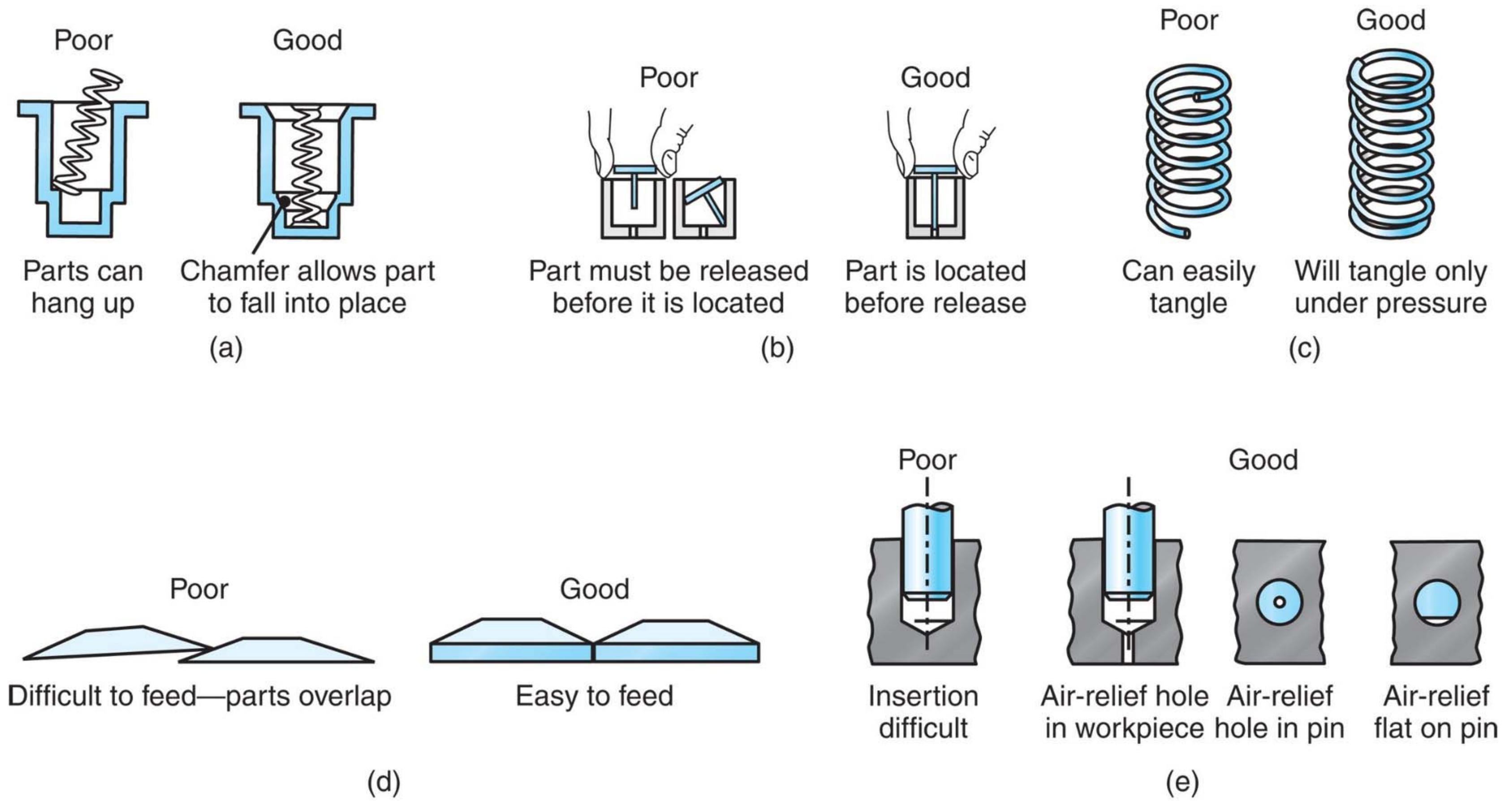

TABLE I.3 General Manufacturing Characteristics of Various Materials

TABLE I.3

General Manufacturing Characteristics of Various Materials

Alloy	Castability	Weldability	Machinability
Aluminum	Excellent	Fair	Excellent–good
Copper	Good–fair	Fair	Good–fair
Gray cast iron	Excellent	Difficult	Good
White cast iron	Good	Very poor	Very poor
Nickel	Fair	Fair	Fair
Steels	Fair	Excellent	Fair
Zinc	Excellent	Difficult	Excellent

The ratings shown depend greatly on the particular material, its alloys, and its processing history.

FIGURE I.4 Cross-sections of baseball bats made of aluminum (top two) and composite material (bottom two).

FIGURE I.5a Schematic illustrations of various casting processes.

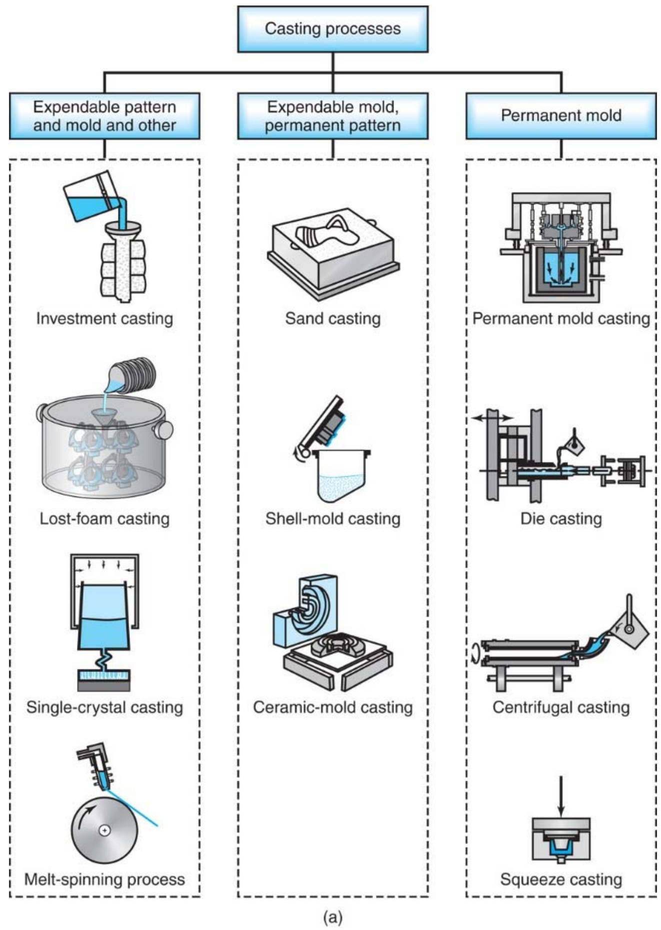

FIGURE I.5b Schematic illustrations of various bulk-deformation processes.

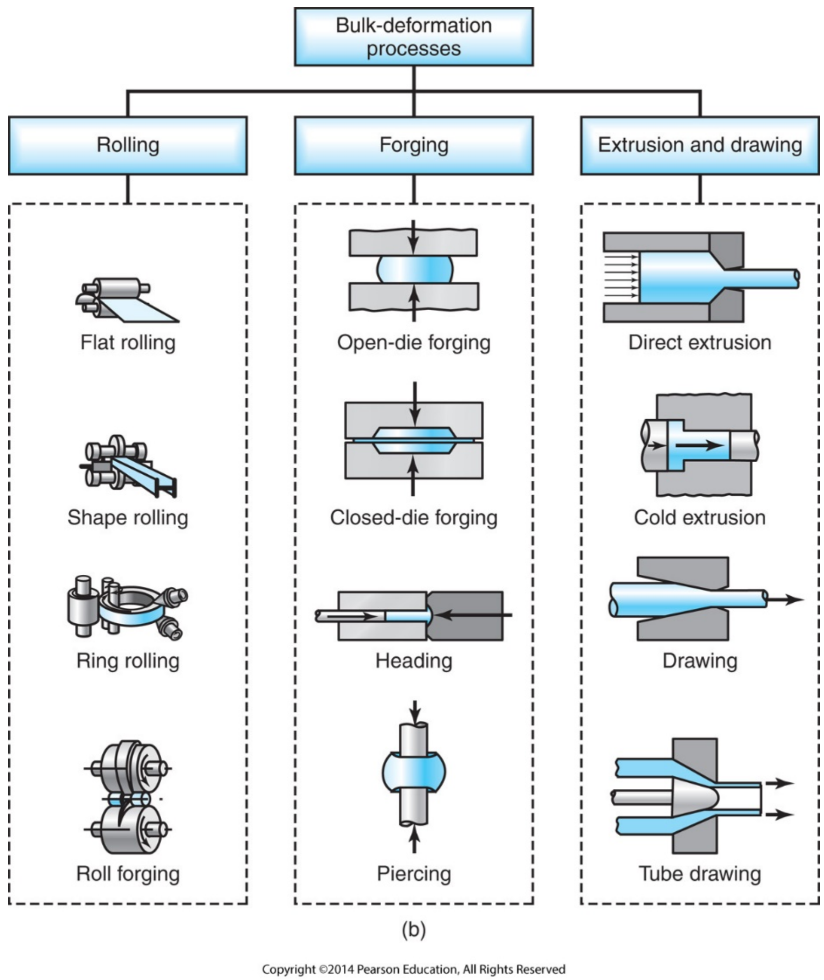

FIGURE I.5c Schematic illustrations of various sheet-metal forming processes.

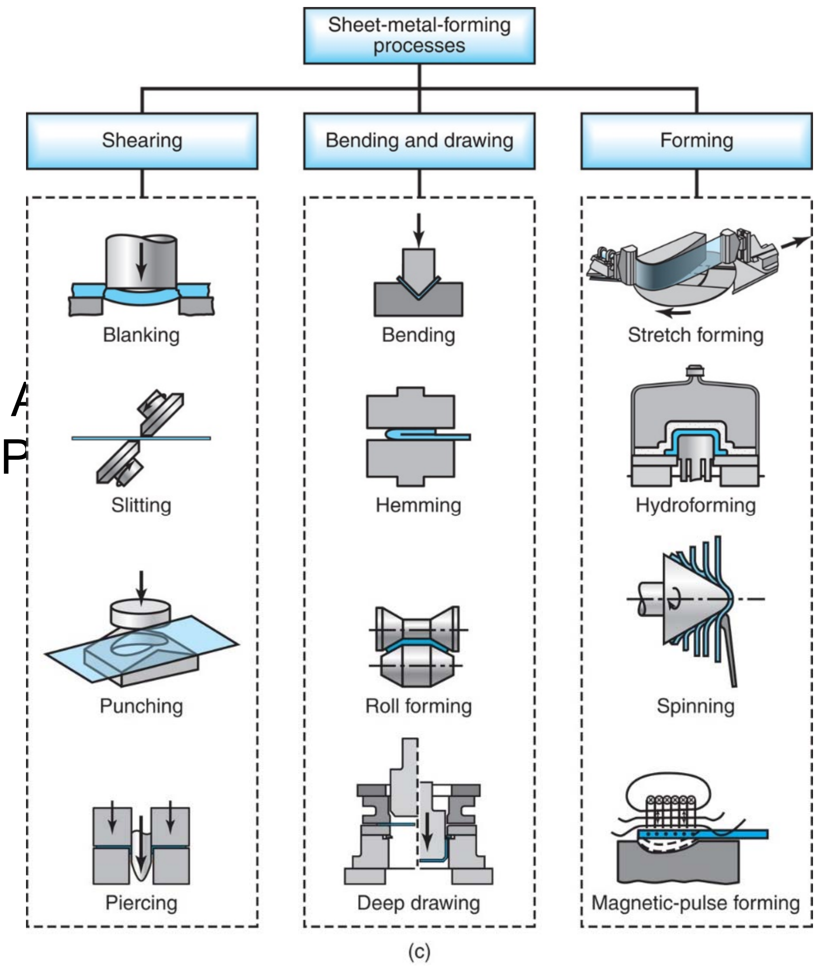

FIGURE I.5d Schematic illustrations of various polymer-processing methods.

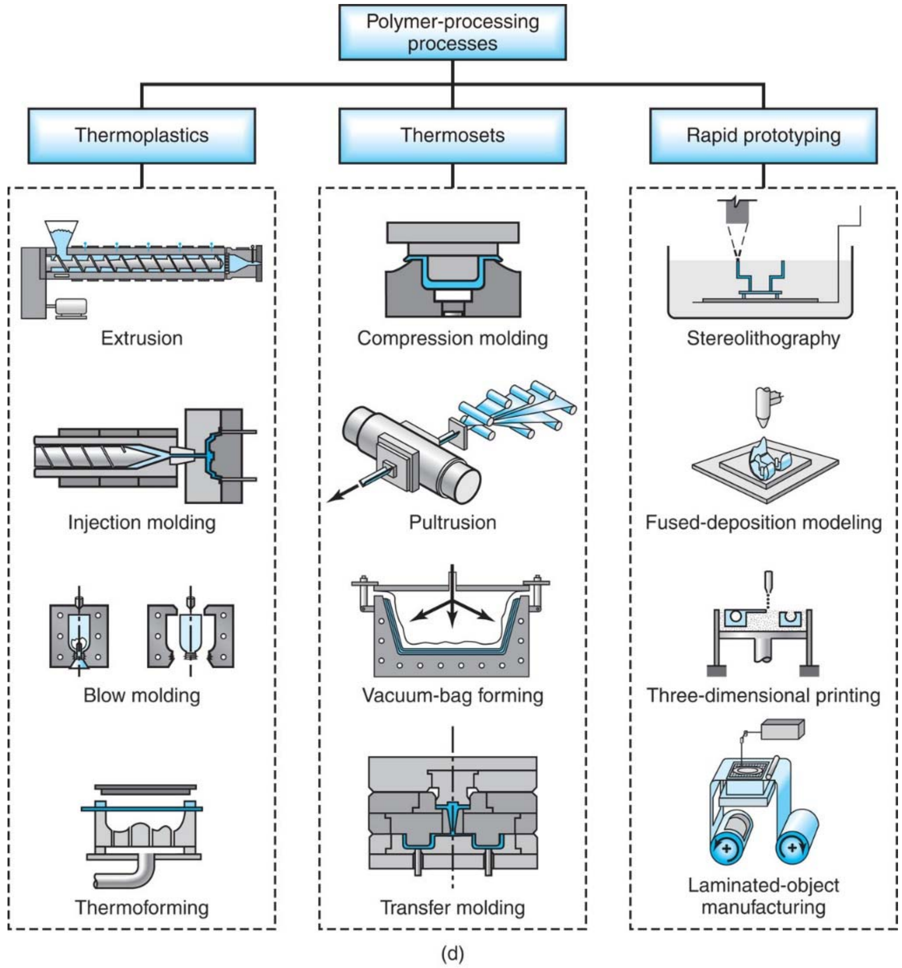

FIGURE I.5e Schematic illustrations of various machining and finishing processes.

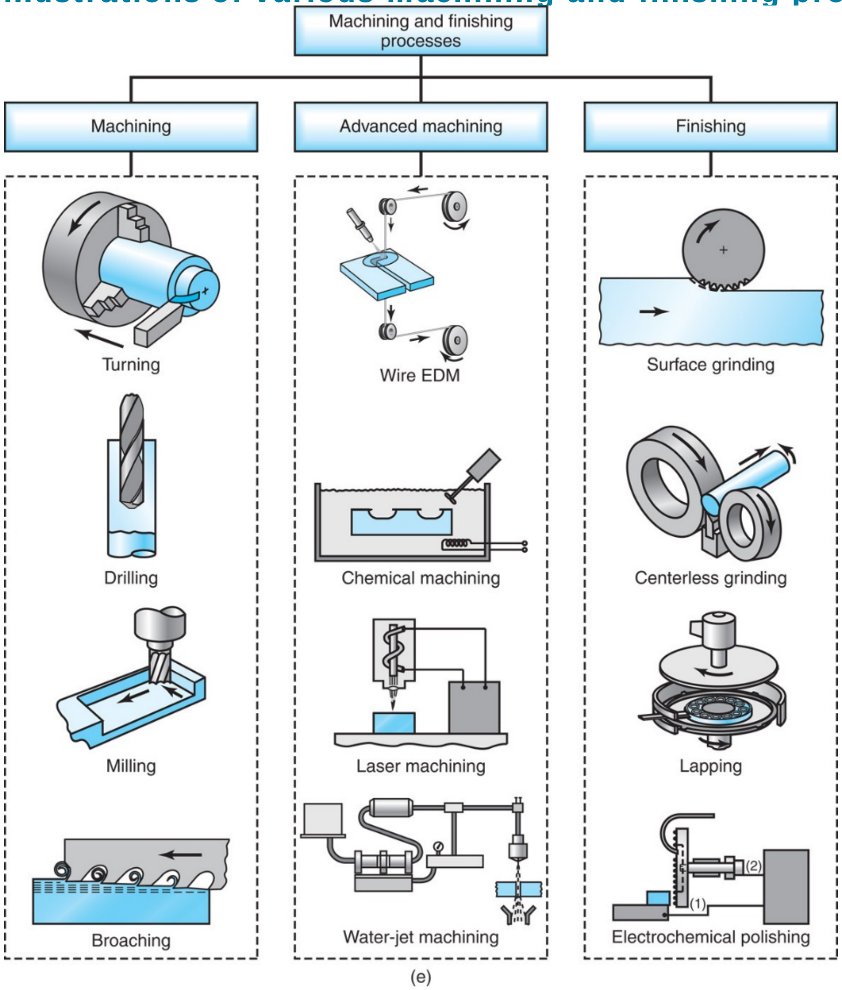

FIGURE I.5f Schematic illustrations of various joining processes.

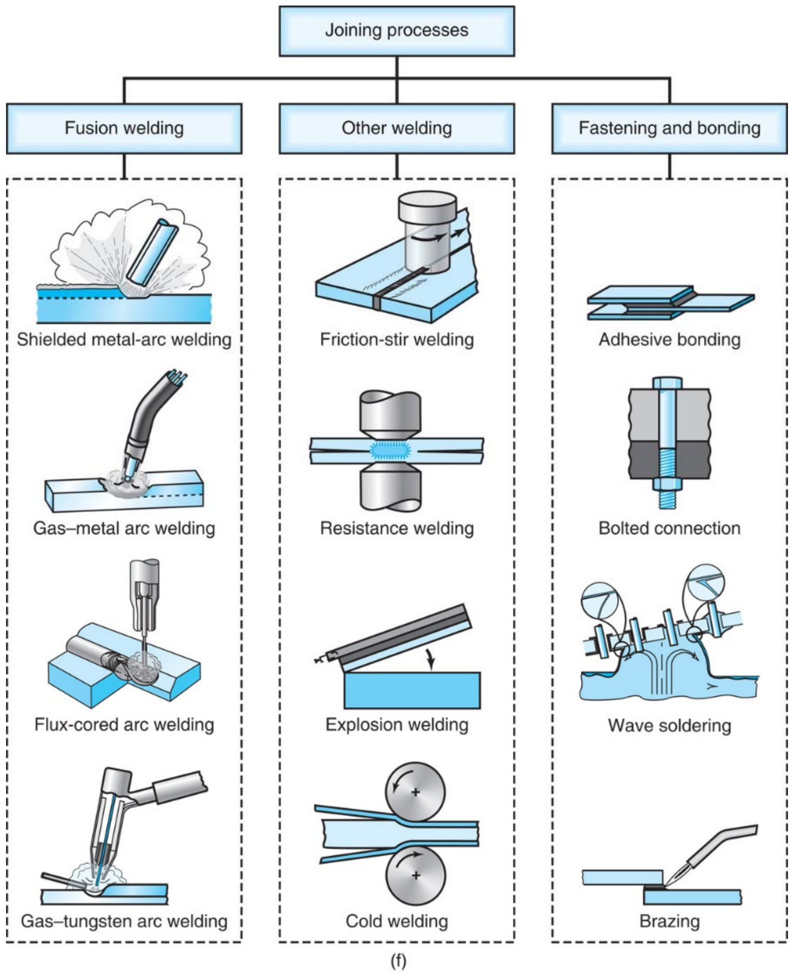

FIGURE I.7 (a) Microscopic gears with dust mite. *Source:* Courtesy of Sandia National Laboratory. Printed with permission; (b) a movable micromirror component of a light sensor; note the scale at the bottom of the figure. *Source:* Courtesy of R. Mueller, University of California at Berkeley.

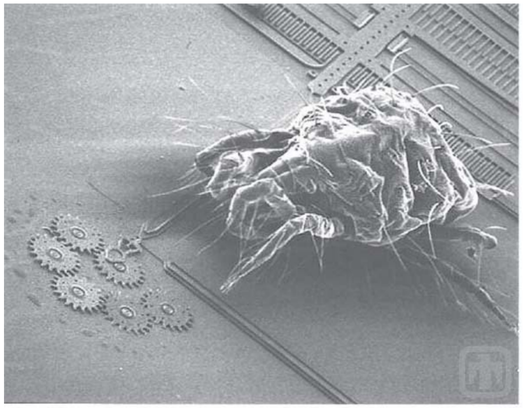

(a)

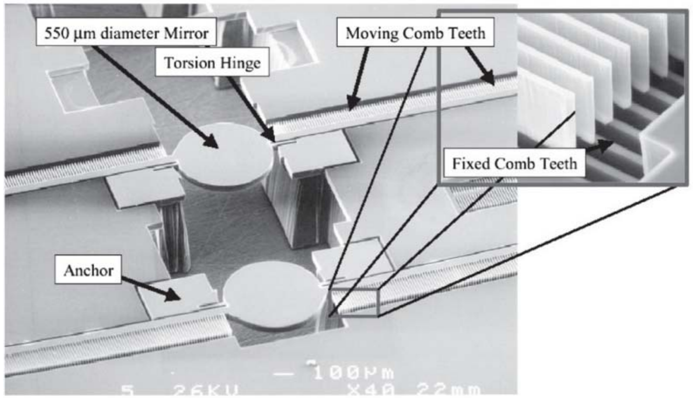

(b)

FIGURE I.8 A saltshaker and pepper mill set. The two metal pieces (at the bottom) for the pepper mill are made by powder metallurgy techniques. ***Source:*** **Metal Powder Industries Federation.**

FIGURE I.9 Automated spot welding of automobile bodies in a mass-production line.

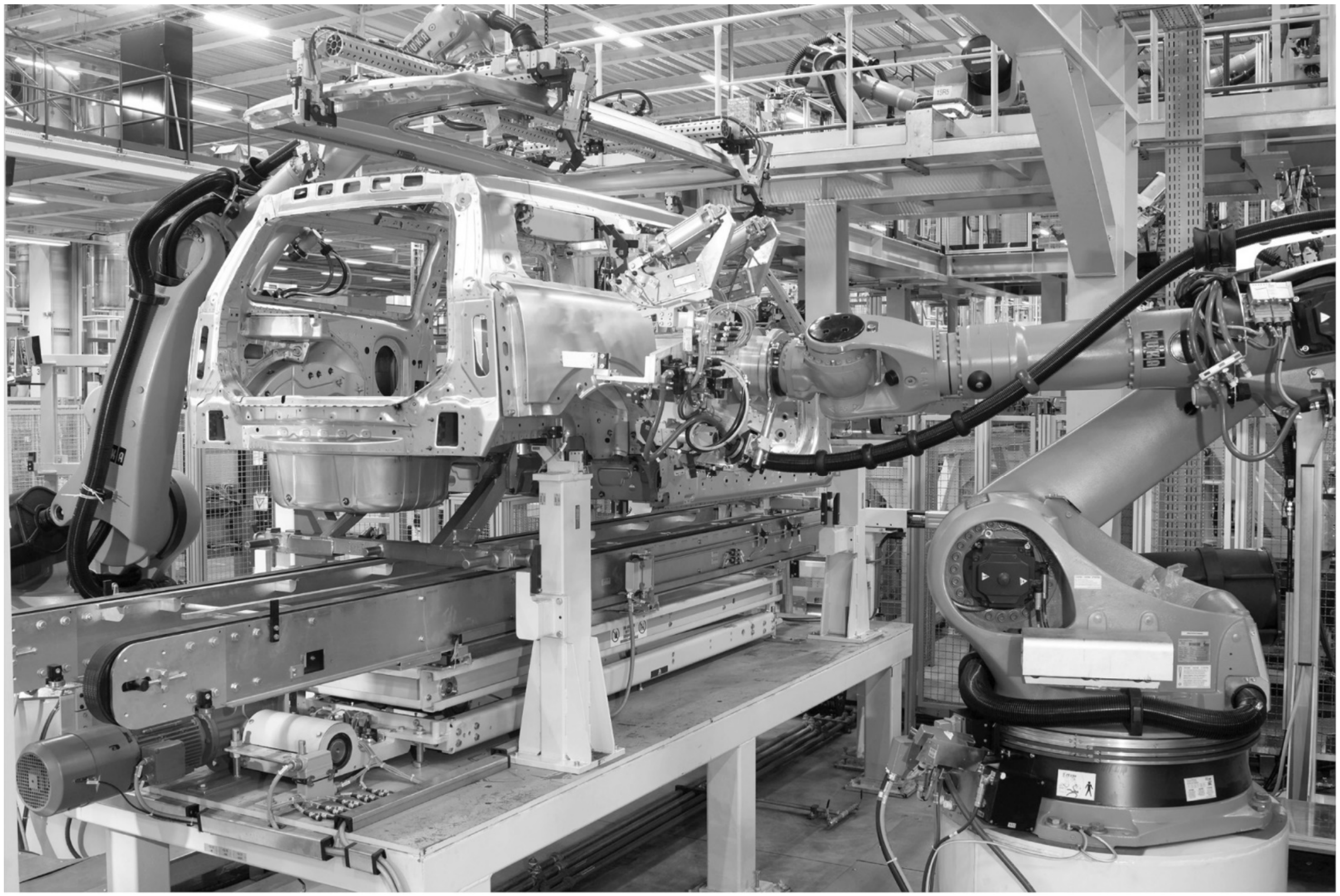

FIGURE I.10a Machining a mold cavity for making sunglasses. Computer model of the sunglasses as designed and viewed on the monitor. *Source:* Courtesy of Mastercam / CNC Software, Inc.

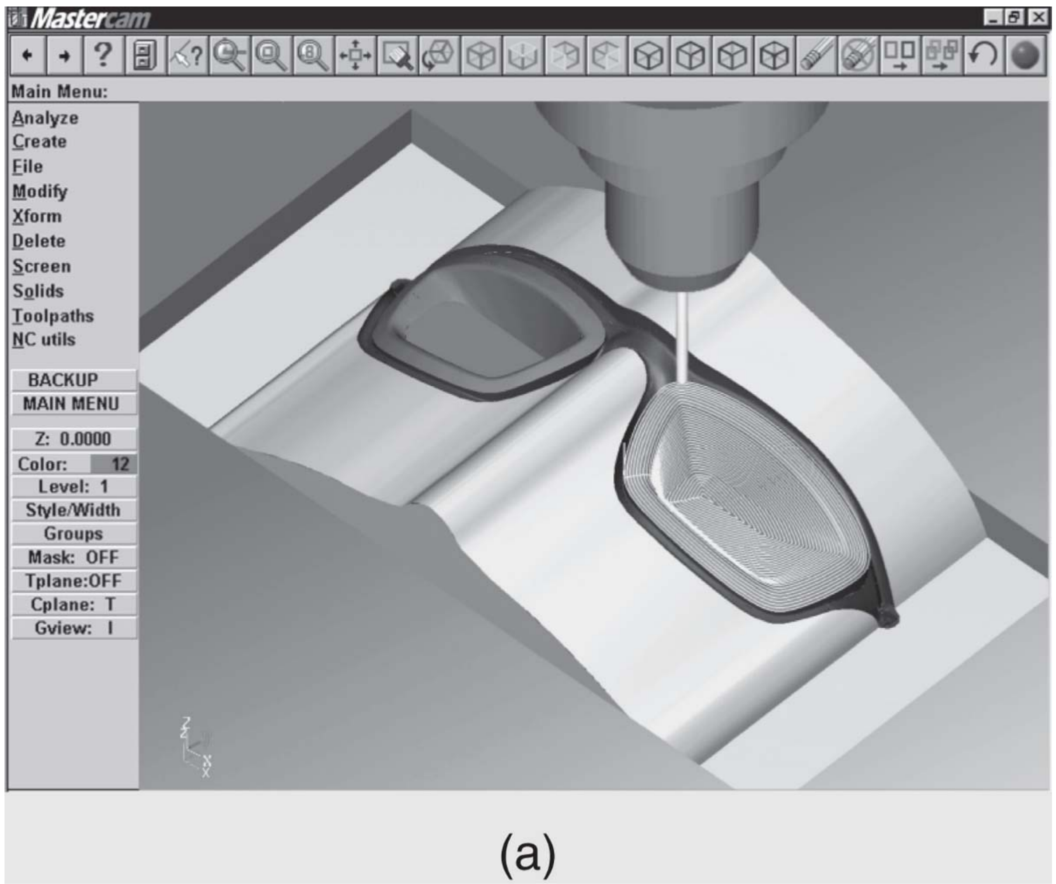

FIGURE I.10b **Machining a mold cavity for making sunglasses. Machining of the die cavity, using a computer numerical-control milling machine.** ***Source:*** **Courtesy of Mastercam / CNC Software, Inc.**

(b)

FIGURE I.10c Machining a mold cavity for making sunglasses. Final product produced from the mold.
Source: **Courtesy of Mastercam / CNC Software, Inc.**

(c)

TABLE I.4 Average Life Expectancy of Various Products

TABLE I.4

Average Life Expectancy of Various Products

Type of product	Life expectancy (years)
U.S. dollar bill	1.5
Personal computer	2
Car battery	4
Hair dryer	5
Automobile	8
Dishwasher	10
Kitchen disposal unit	10
Vacuum cleaner	10
Water heater (gas)	12
Clothes dryer (gas)	13
Clothes washer	13
Air-conditioning unit (central)	15
Manufacturing cell	15
Refrigerator	17
Furnace (gas)	18
Machinery	30
Nuclear reactor	40

Note: Significant variations can be expected, depending on the quality of the product and how well it has been maintained.

TABLE I.5 Relative Cost of Repair at Various Stages of Product Development and Sale

TABLE I.5

Relative Cost of Repair at Various Stages of Product Development and Sale

Stage	Relative cost of repair
When the part is being made	1
Subassembly of the product	10
Assembly of the product	100
Product at the dealership	1000
Product at the customer	10,000

TABLE I.6 Typical Cost Breakdown in Manufacturing

TABLE I.6

Typical Cost Breakdown in Manufacturing	
Design	5%
Materials	50%
Manufacturing	
Direct labor	15%
Indirect labor	30%

TABLE I.7 Approximate Relative Hourly Compensation for Workers in Manufacturing in 2010 (United States = 100)

TABLE I.7

Approximate Relative Hourly Compensation for Workers in Manufacturing in 2010 (United States = 100)

Norway	166	Italy	96
Switzerland	153	Japan	92
Belgium	146	Spain	76
Denmark	131	New Zealand	59
Germany	126	Israel	58
Sweden	126	Singapore	55
Finland	122	Korea (South)	48
Austria	118	Argentina, Slovakia	36
Netherlands, Australia	118	Portugal	34
France	117	Czech Republic	33
Ireland	104	Poland	23
United States	100	Mexico	18
Canada	97	China, India, Philippines	6

Note: Compensation can vary significantly with benefits. Data for China and India are estimates, they use different statistical measures of compensation, and are provided here for comparison purposes only.
Source: U.S. Department of Labor.

FIGURE I.1 An outline of the topics described in Part I.

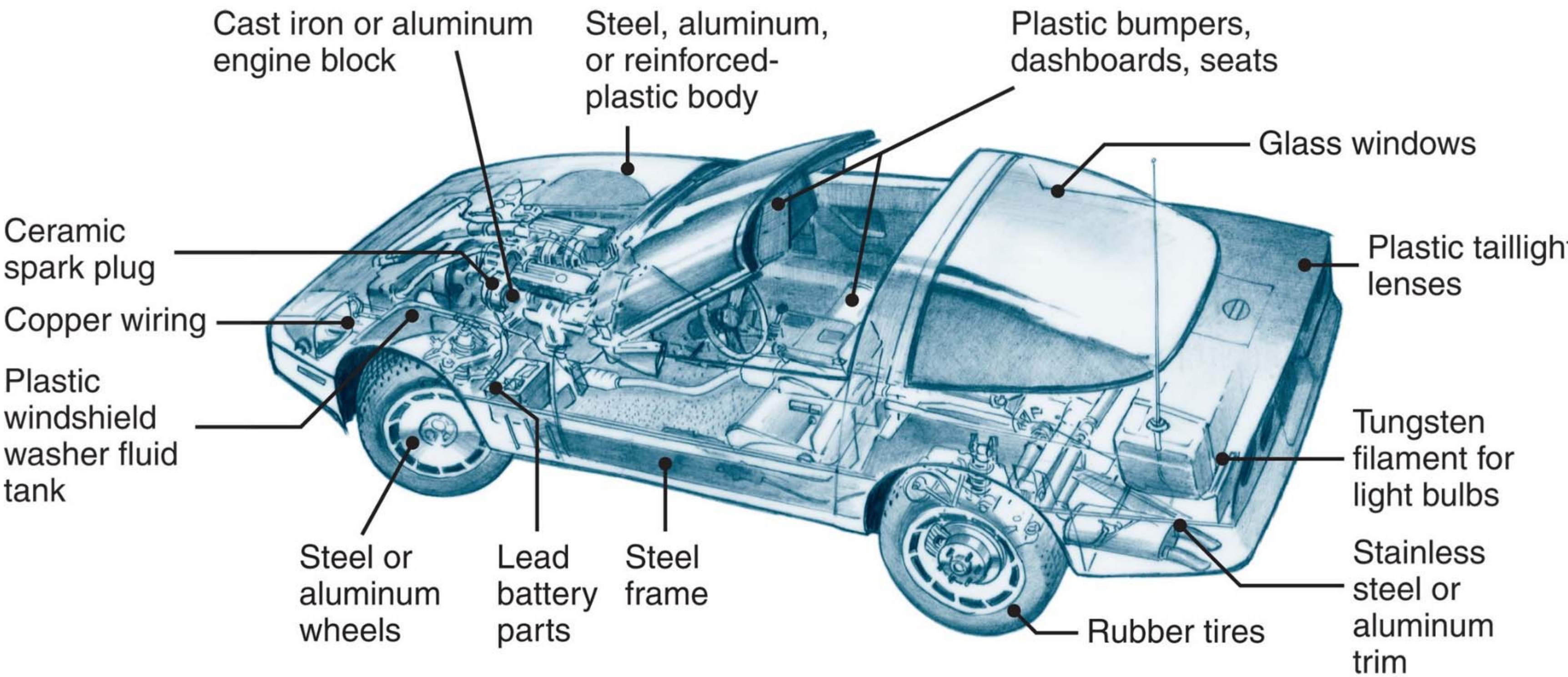

FIGURE I.2 An outline of the engineering materials described in Part I.

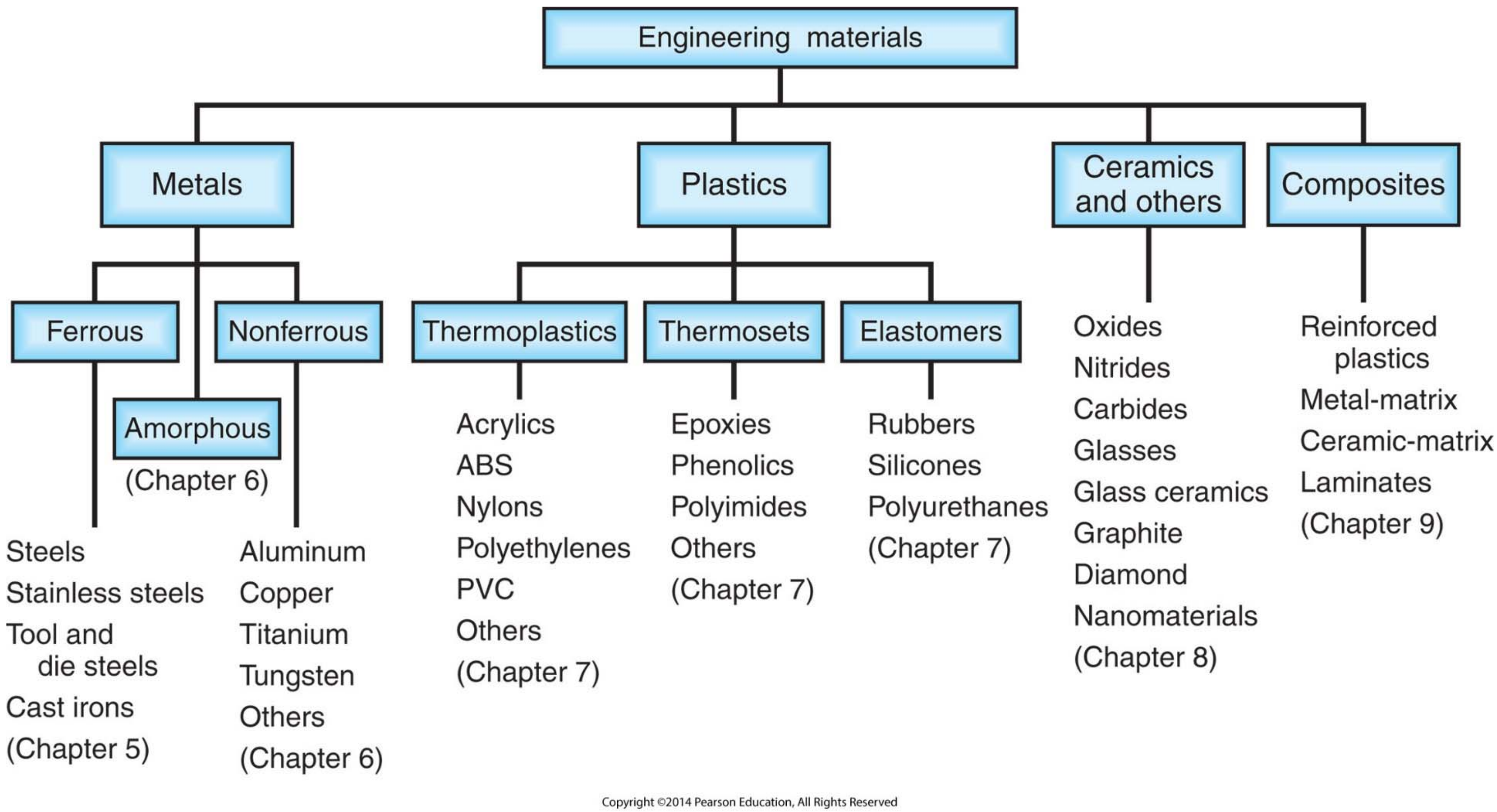

FIGURE I.3 An outline of the behavior and the manufacturing properties of materials described in Part I.

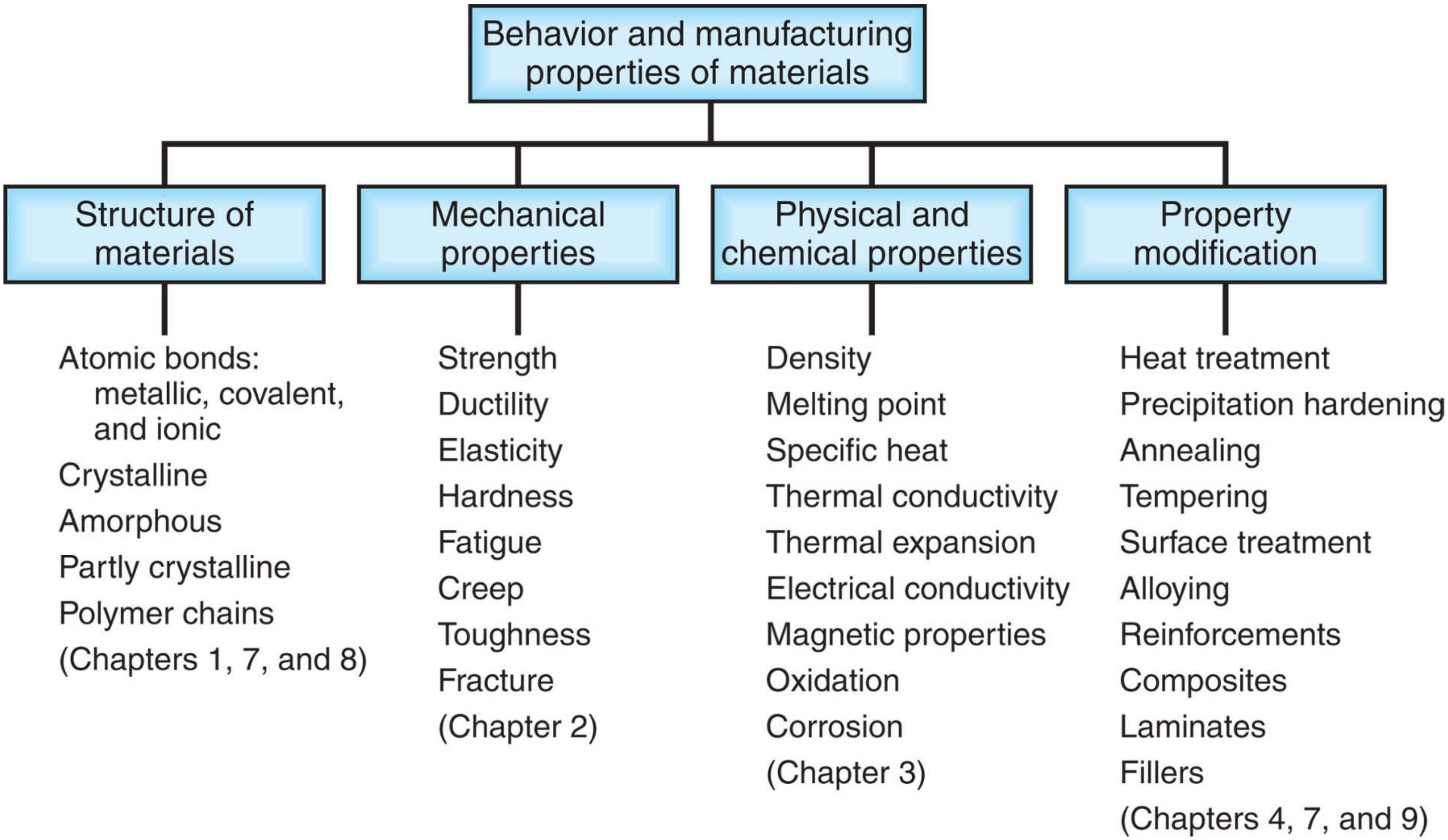

Figure 1.1

Turbine blades for jet engines, manufactured by three different methods: left: conventionally cast; center: directionally solidified, with columnar grains as can be seen from the vertical streaks, and right: single crystal. Although more expensive, single-crystal blades have properties at high temperatures that are superior to those of other blades.

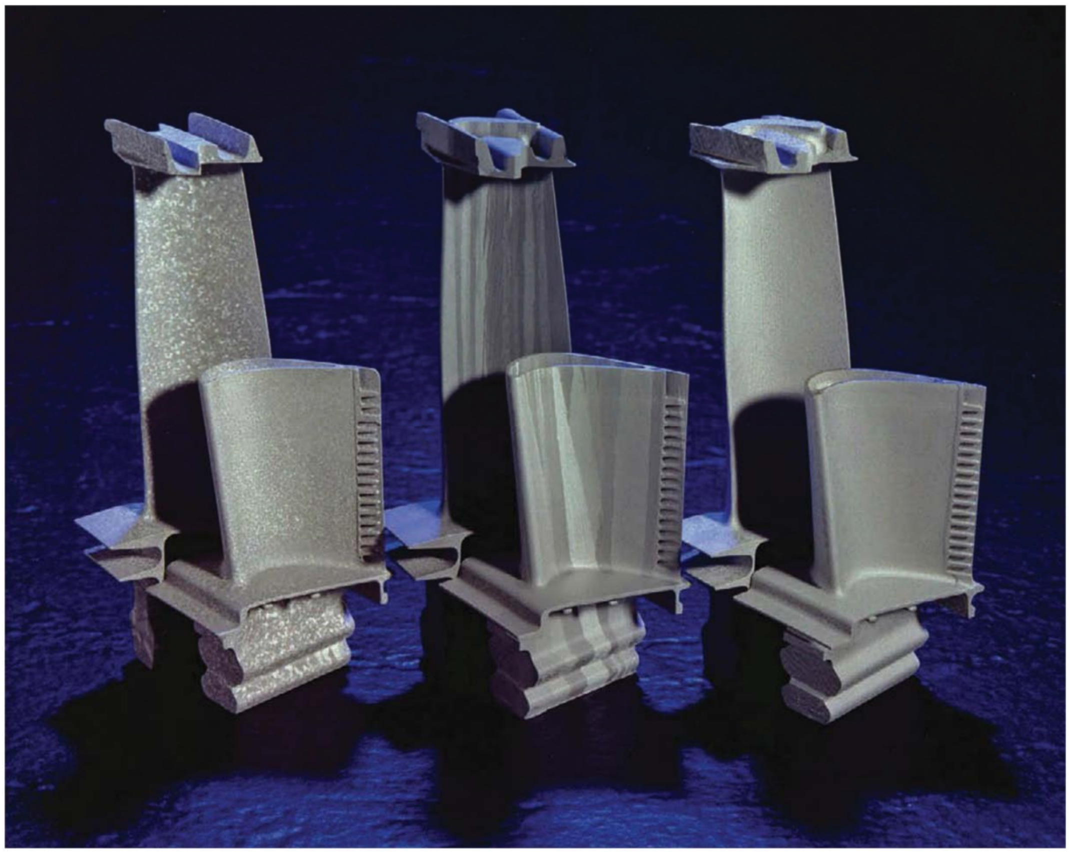

Source: Courtesy of NASA.

Figure 1.2

An outline of the topics described in Chapter 1.

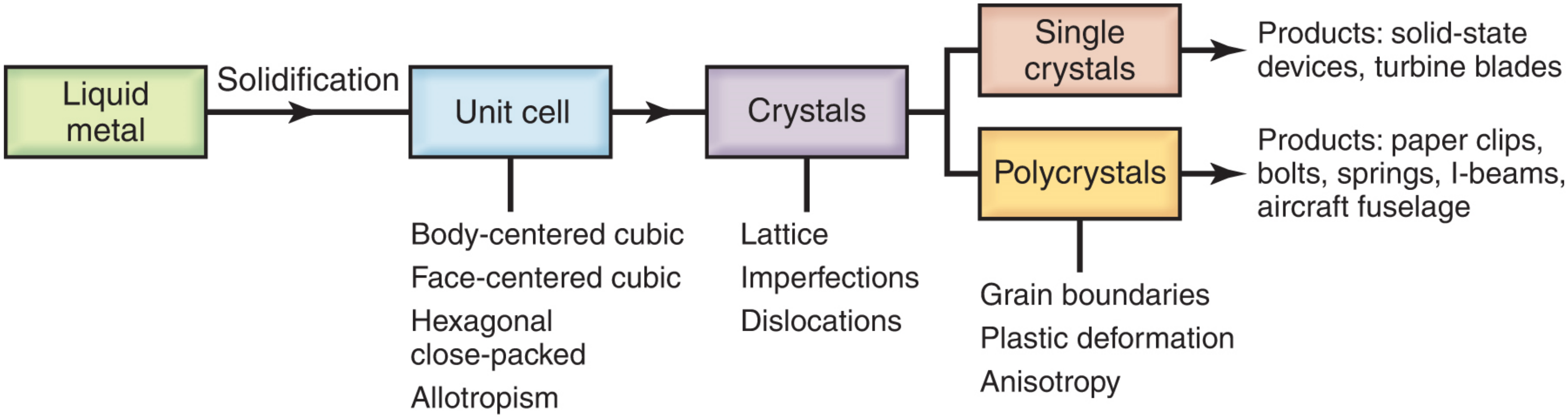

Figure 1.3

The body-centered cubic (bcc) crystal structure: (a) hard-ball model.

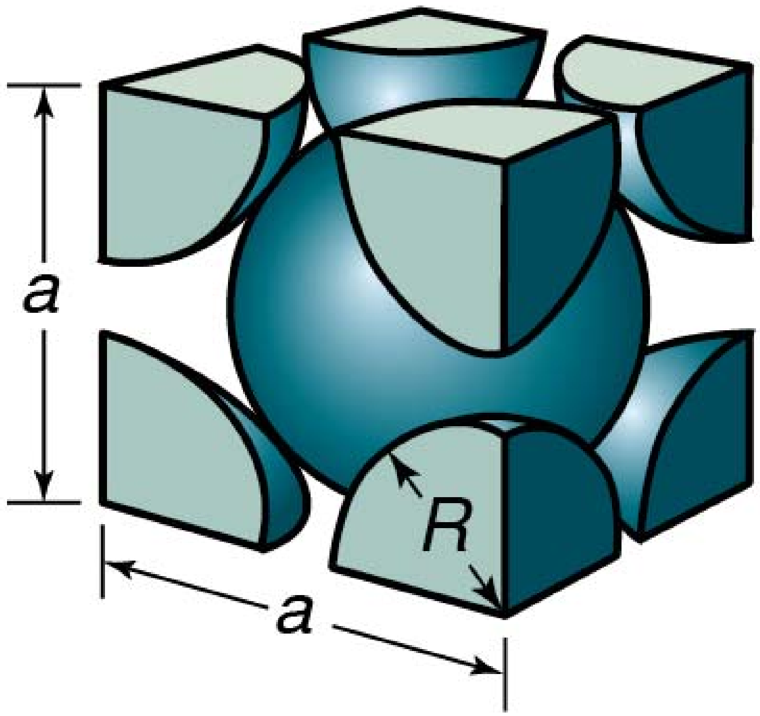

(a)

Figure 1.4

The face-centered cubic (fcc) crystal structure: (a) hard-ball model.

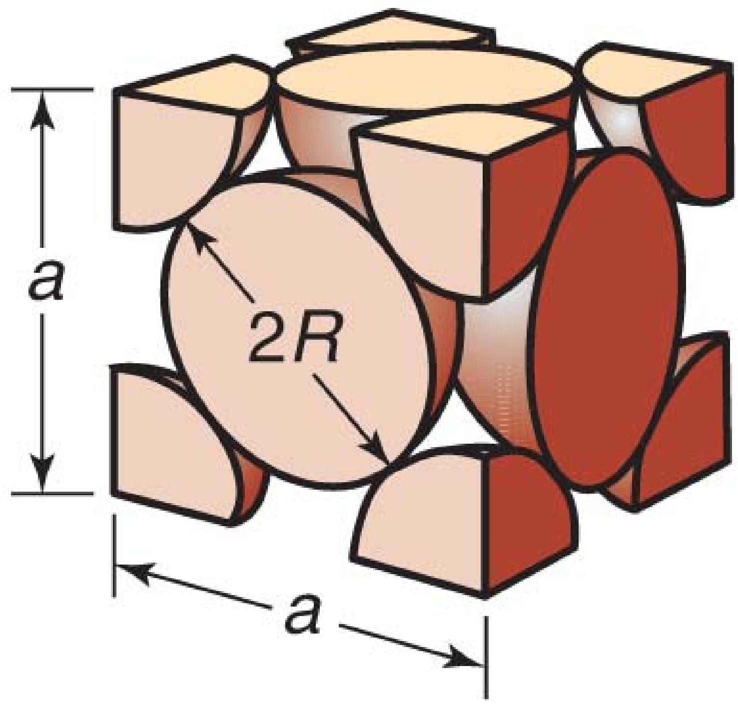

(a)

Pearson

Figure 1.5

The hexagonal close-packed (hcp) crystal structure: (a) unit cell.

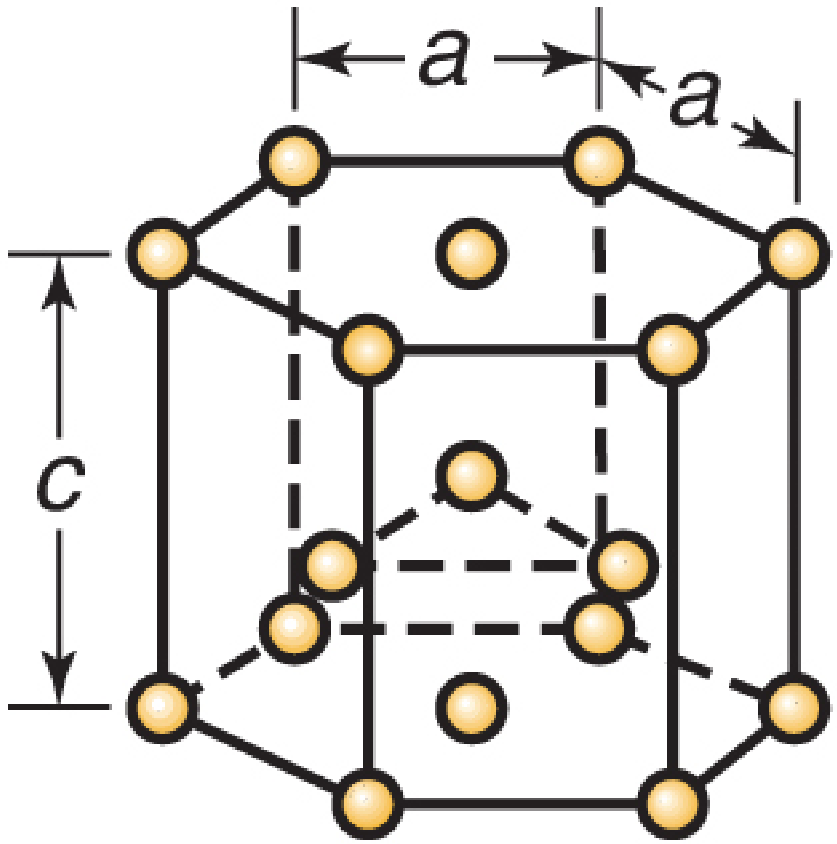

(a)

Pearson

Figure 1.6 (1 of 2)

Permanent deformation of a single crystal under a tensile load. The highlighted grid of atoms emphasizes the motion that occurs within the lattice. (a) Deformation by slip. The *b*/*a* ratio influences the magnitude of the shear stress required to cause slip.

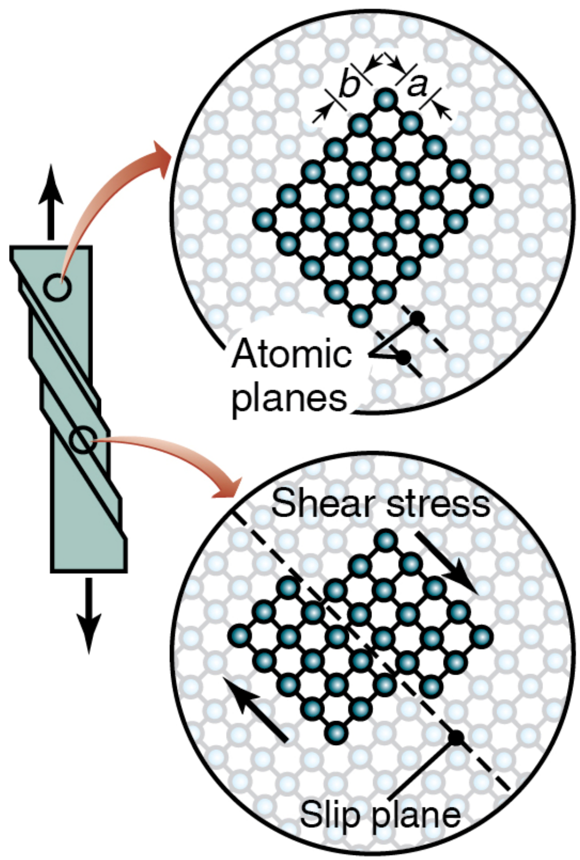

(a)

Figure 1.6 (2 of 2)

Permanent deformation of a single crystal under a tensile load. The highlighted grid of atoms emphasizes the motion that occurs within the lattice. (b) Deformation by twinning, involving the generation of a “twin” around a line of symmetry subjected to shear. Note that the tensile load results in a shear stress in the plane illustrated.

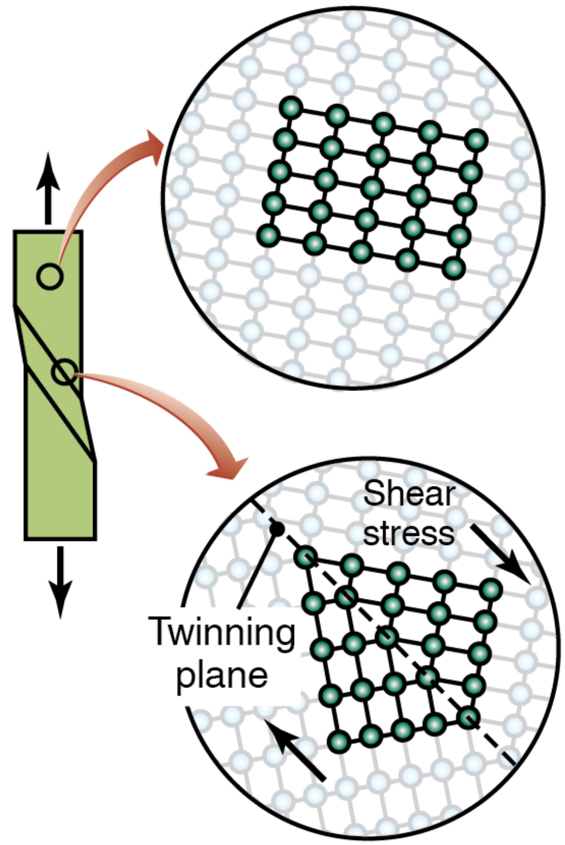

(b)

Figure 1.7

Schematic illustration of slip lines and slip bands in a single crystal (grain) subjected to a shear stress. A slip band consists of a number of slip planes. The crystal at the center of the upper illustration is an individual grain surrounded by several other grains.

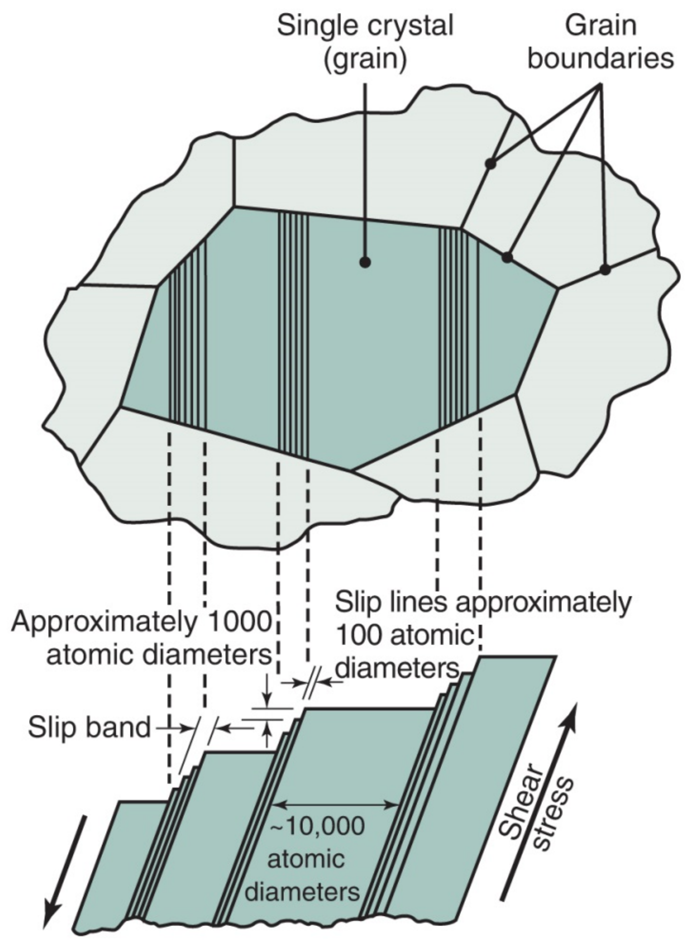

Pearson

Figure 1.8

Schematic illustration of types of defects in a single-crystal lattice: self-interstitial, vacancy, interstitial, and substitutional.

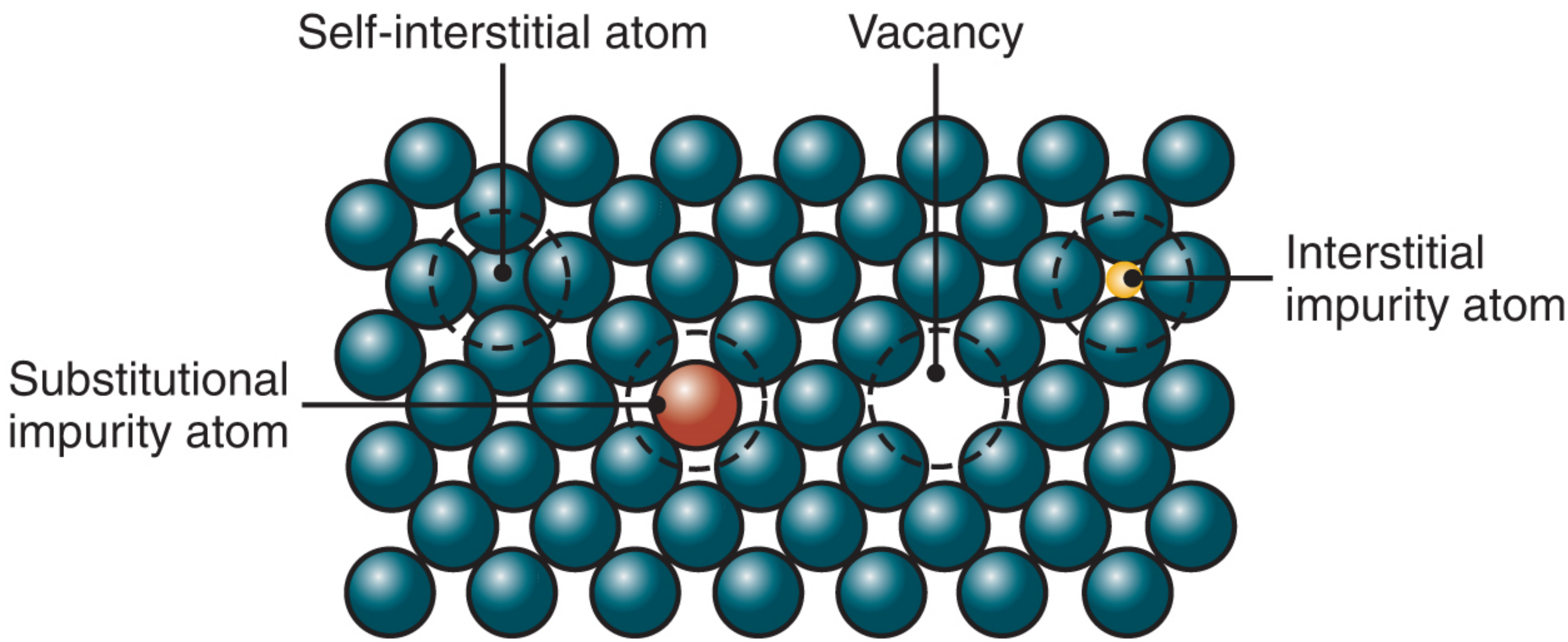

Figure 1.9

Types of dislocations in a single crystal: (a) edge dislocation and (b) screw dislocation.

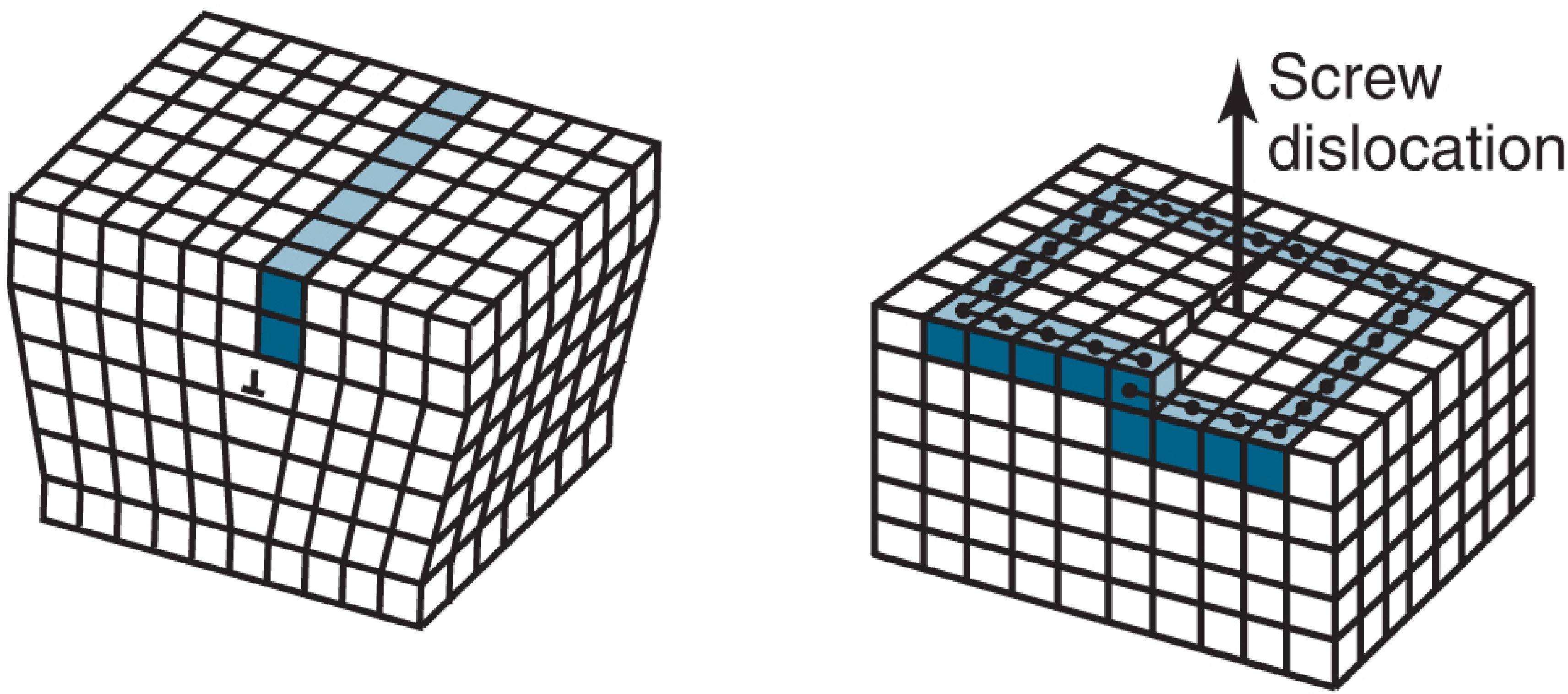

(a) (b)

Figure 1.10

Movement of an edge dislocation across the crystal lattice under a shear stress. Dislocations help explain why the actual strength of metals is much lower than that predicted by theory.

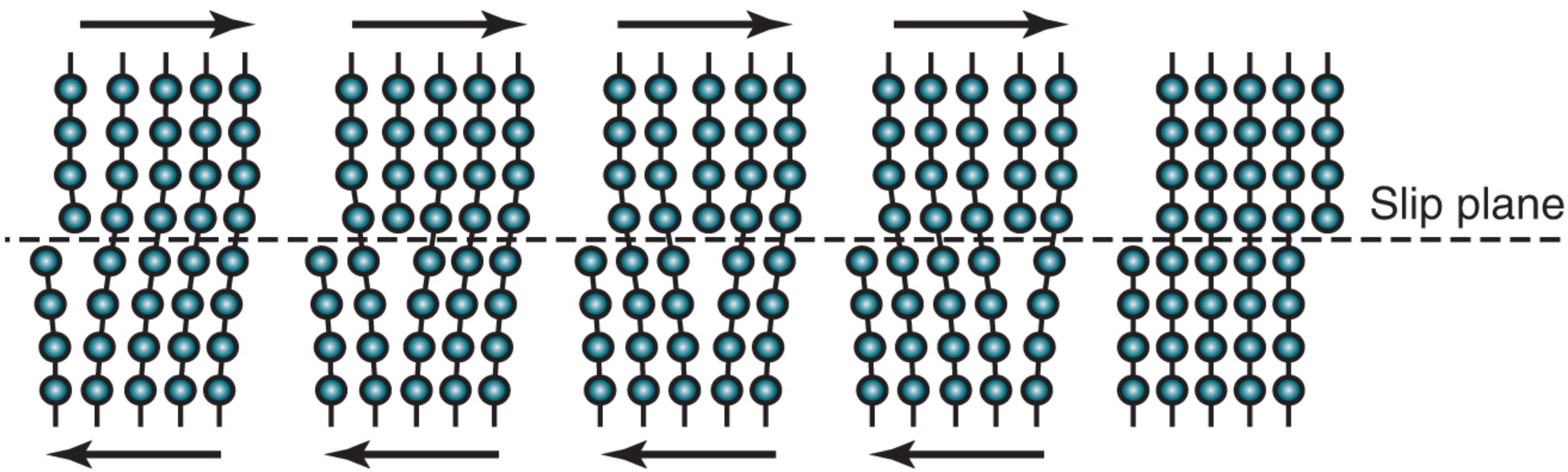

Figure 1.11 (1 of 4)

Schematic illustration of the stages during the solidification of molten metal; each small square represents a unit cell. (a) Nucleation of crystals at random sites in the molten metal; note that the crystallographic orientation of each site is different.

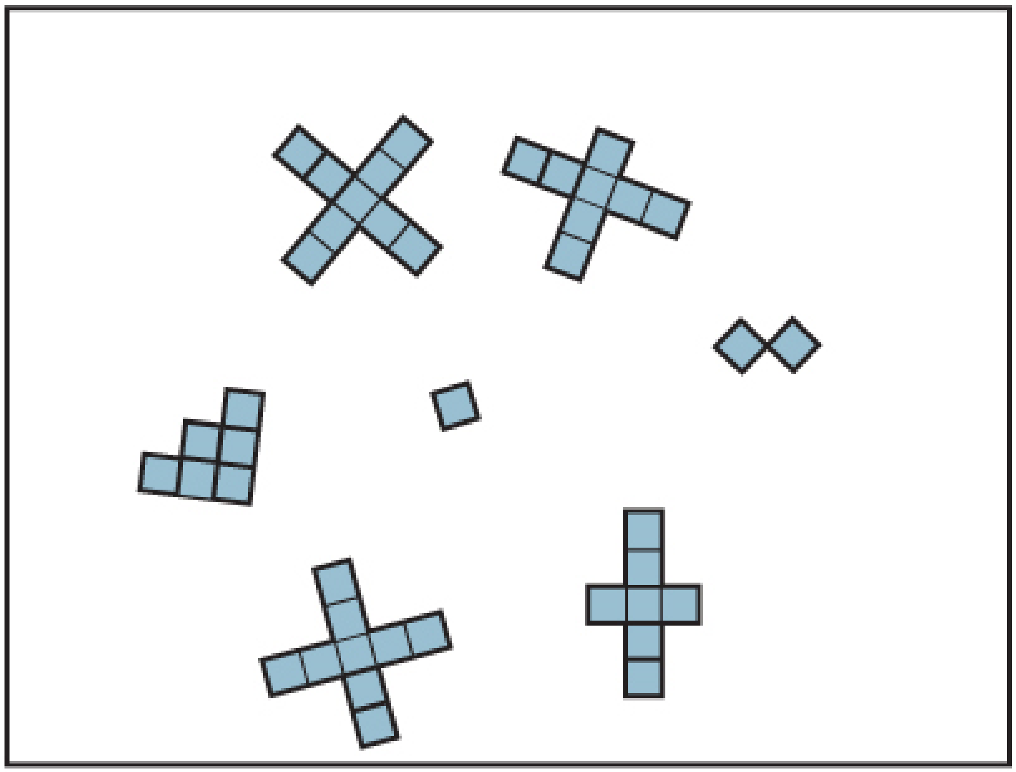

(a)

Pearson

Figure 1.11 (2 of 4)

Schematic illustration of the stages during the solidification of molten metal; each small square represents a unit cell. (b) Growth of crystals as solidification continues.

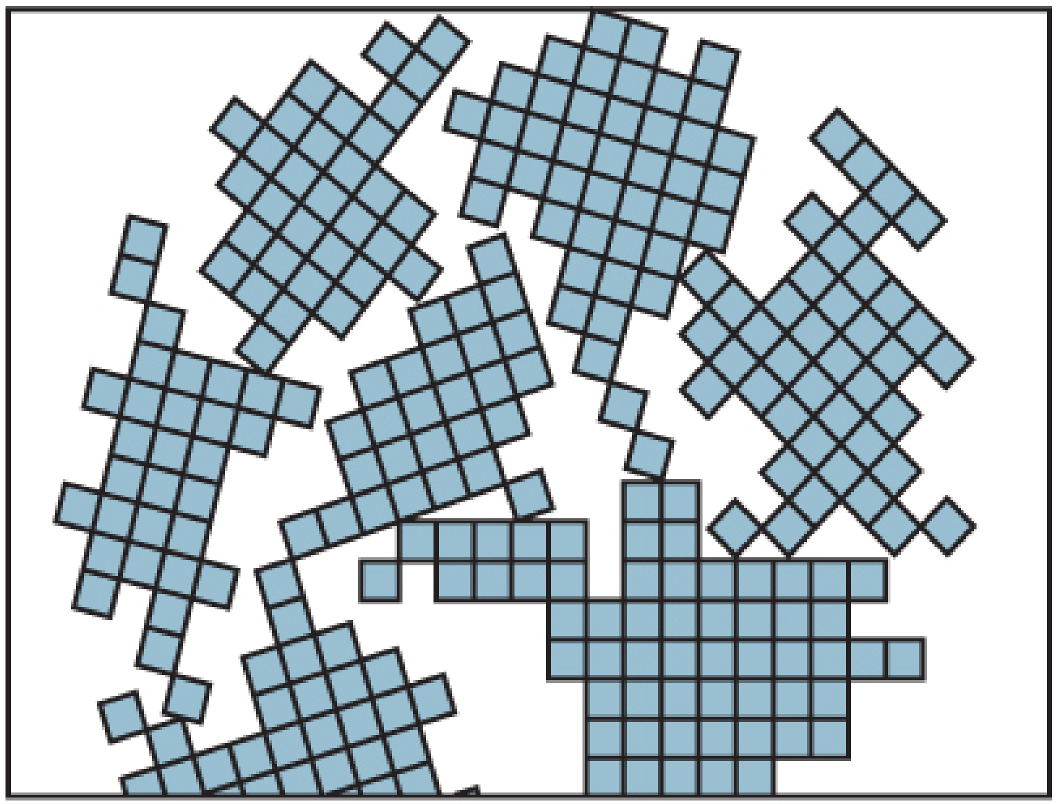

(b)

Pearson

Figure 1.11 (3 of 4)

Schematic illustration of the stages during the solidification of molten metal; each small square represents a unit cell. (c) Growth of crystals as solidification continues.

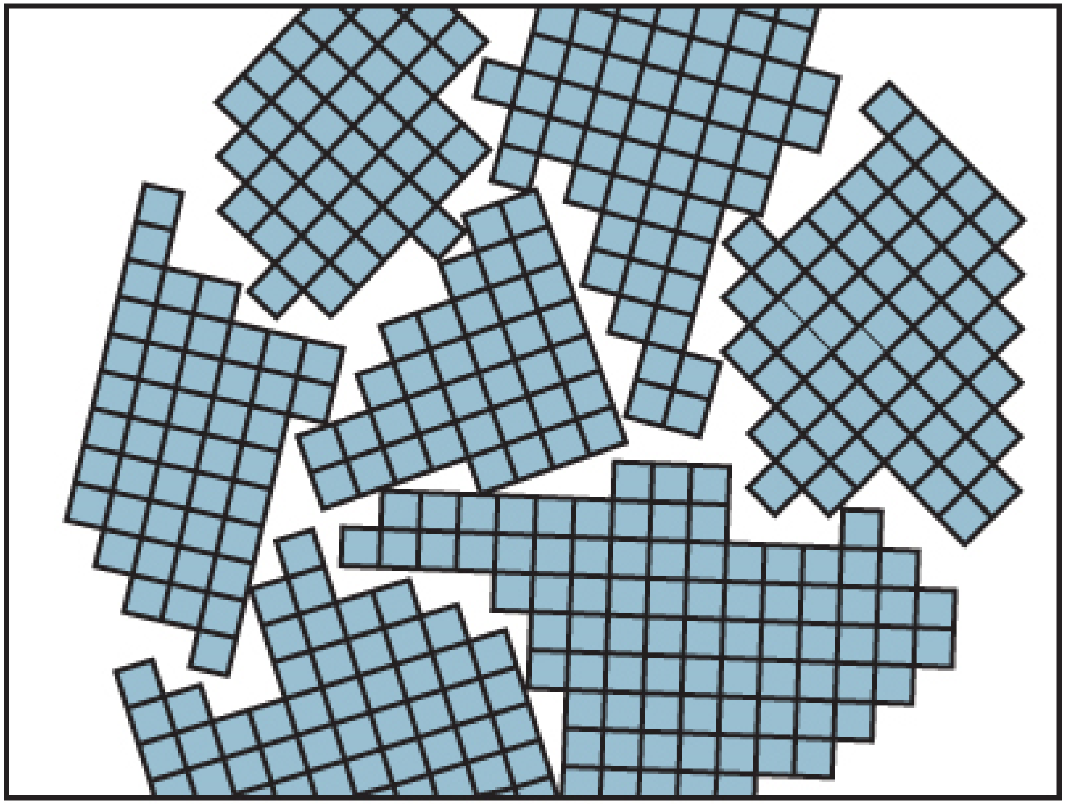

(c)

Figure 1.11 (4 of 4)

Schematic illustration of the stages during the solidification of molten metal; each small square represents a unit cell. (d) Solidified metal, showing individual grains and grain boundaries; note the different angles at which neighboring grains meet each other.

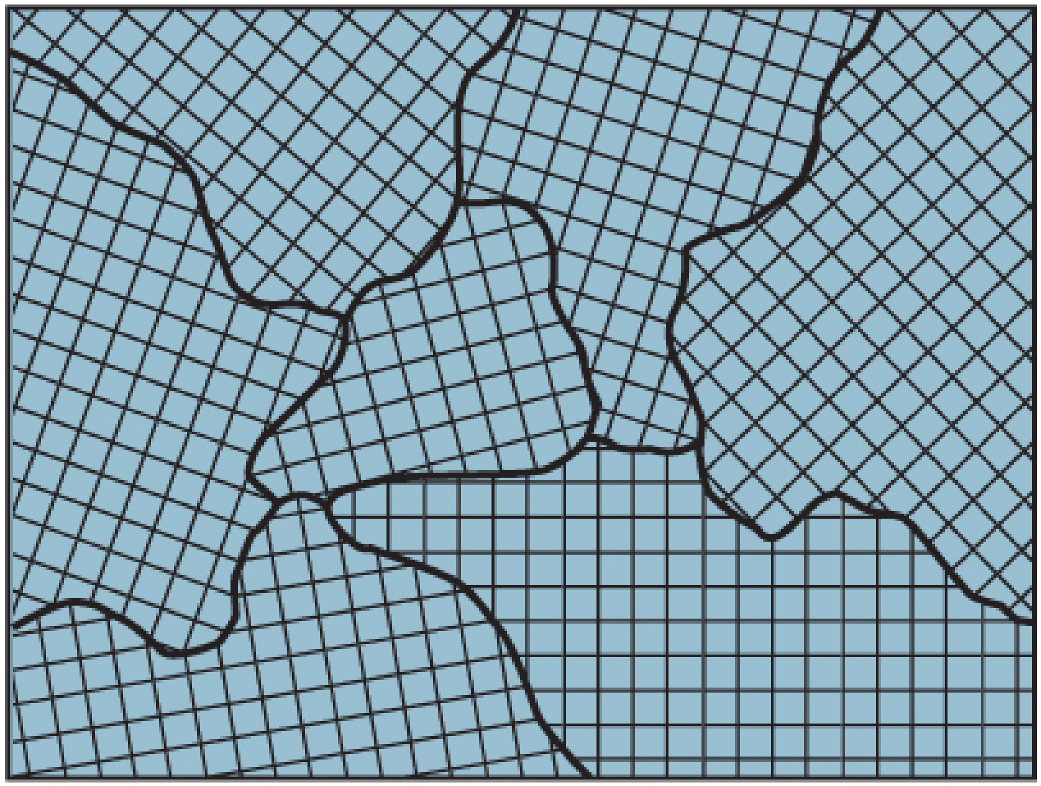

(d)

Pearson

Table 1.1

Grain Sizes.

ASTM No.	Grains/mm^2	Grains/mm^3
−3	1	0.7
−2	2	2
−1	4	5.6
0	8	16
1	16	45
2	32	128
3	64	360
4	128	1020
5	256	2900
6	512	8200
7	1024	23,000
8	2048	65,000
9	4096	185,000
10	8200	520,000
11	16,400	1,500,000

Figure 1.12 (1 of 2)

Plastic deformation of idealized (equiaxed) grains in a specimen subjected to compression (such as occurs in the forging or rolling of metals): (a) before deformation.

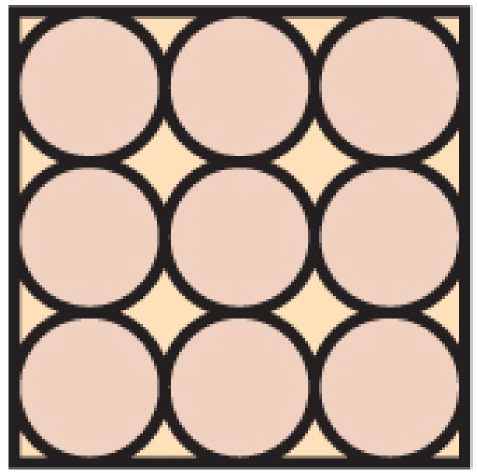

(a)

Figure 1.12 (2 of 2)

Plastic deformation of idealized (equiaxed) grains in a specimen subjected to compression (such as occurs in the forging or rolling of metals): (b) after deformation. Note the alignment of grain boundaries along a horizontal direction; this effect is known as *preferred orientation.*

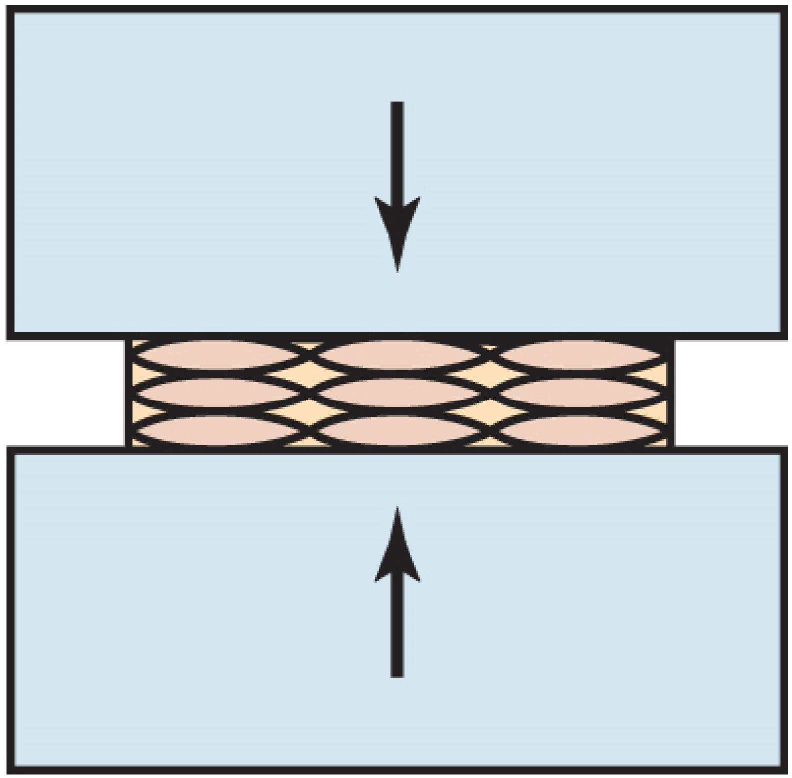

(b)

Figure 1.13 (1 of 2)

(a) Schematic illustration of a crack in sheet metal that has been subjected to bulging (caused, for example, by pushing a steel ball against the sheet). Note the orientation of the crack with respect to the rolling direction of the sheet; this sheet is anisotropic.

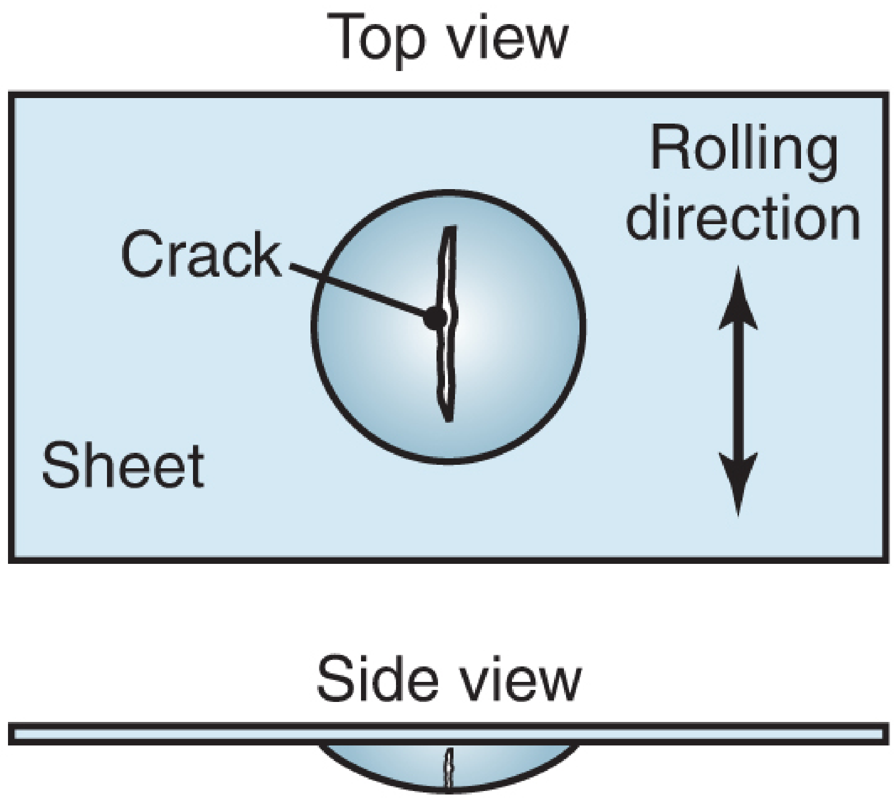

(a)

Figure 1.13 (2 of 2)

(b) Aluminum sheet with a crack (vertical dark line at the center) developed in a bulge test; the rolling direction of the sheet was vertical.

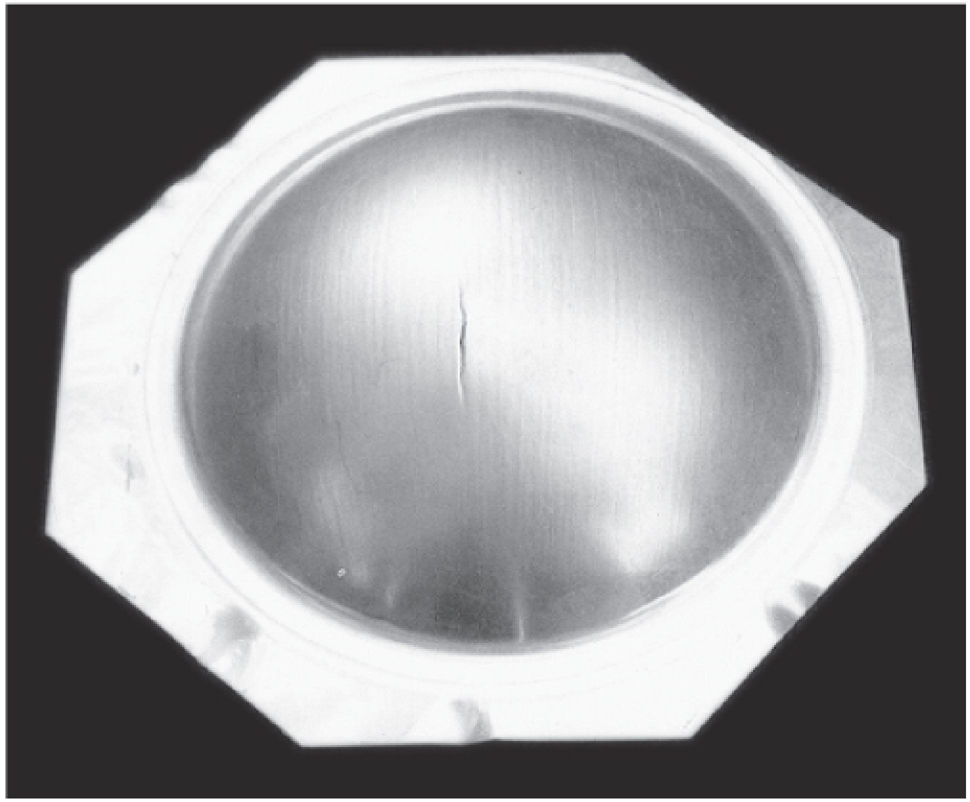

(b)

Source: After J.S. Kallend, Illinois Institute of Technology.

Figure 1.14

Schematic illustration of the effects of recovery, recrystallization, and grain growth on mechanical properties and on the shape and size of grains. Note the formation of small new grains during recrystallization.

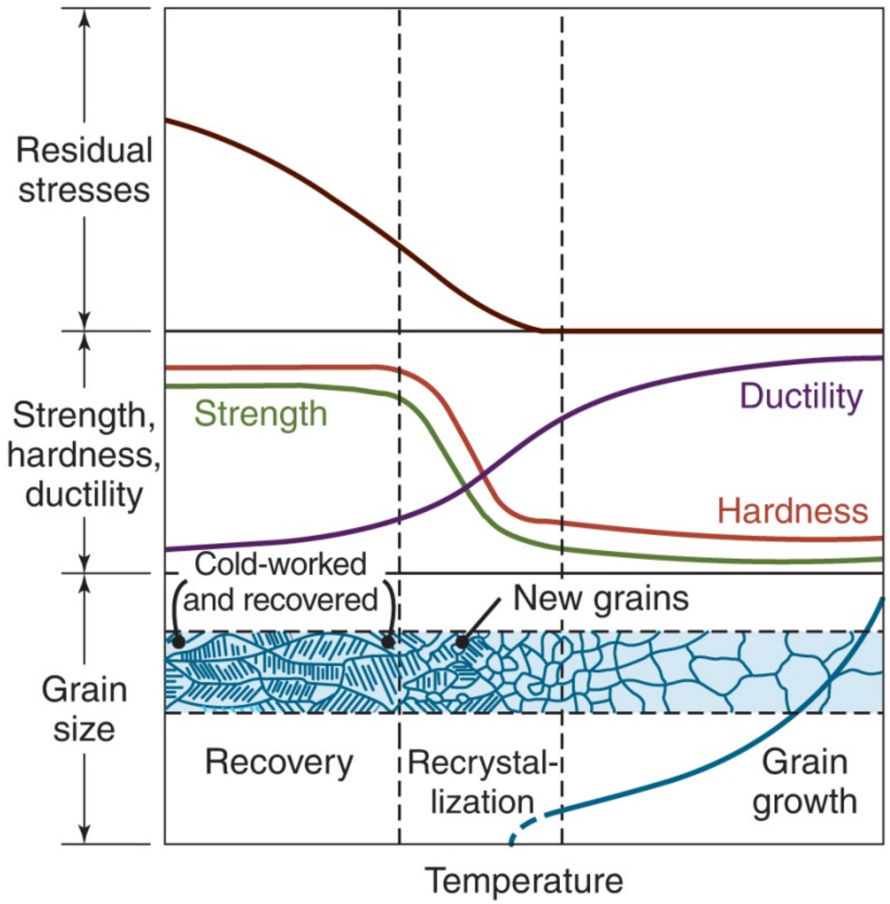

Table 1.2

Homologous Temperature Ranges for Various Processes.

Process	T/T_m
Cold working	<0.3
Warm working	0.3–0.5
Hot working	>0.6

Table 2.1

Relative Mechanical Properties of Various Materials at Room Temperature, in Decreasing Order. Metals Are in Their Alloy Form.

Strength	Hardness	Toughness	Stiffness	Strength/Density
Glass fibers	Diamond	Ductile metals	Diamond	Reinforced plastics
Carbon fibers	Cubic boron nitride	Reinforced plastics	Carbides	Titanium
Kevlar fibers	Carbides	Thermoplastics	Tungsten	Steel
Carbides	Hardened steels	Wood	Steel	Aluminum
Molybdenum	Titanium	Thermosets	Copper	Magnesium
Steels	Cast irons	Ceramics	Titanium	Beryllium
Tantalum	Copper	Glass	Aluminum	Copper
Titanium	Thermosets		Ceramics	Tantalum
Copper	Magnesium		Reinforced plastics	
Reinforced thermosets	Thermoplastics		Wood	
Reinforced thermoplastics	Tin		Thermosets	
Thermoplastics	Lead		Thermoplastics	
Lead			Rubbers	

Pearson

Figure 2.1 (1 of 2)

(a) A standard tensile-test specimen before and after pulling, showing original and final gage lengths.

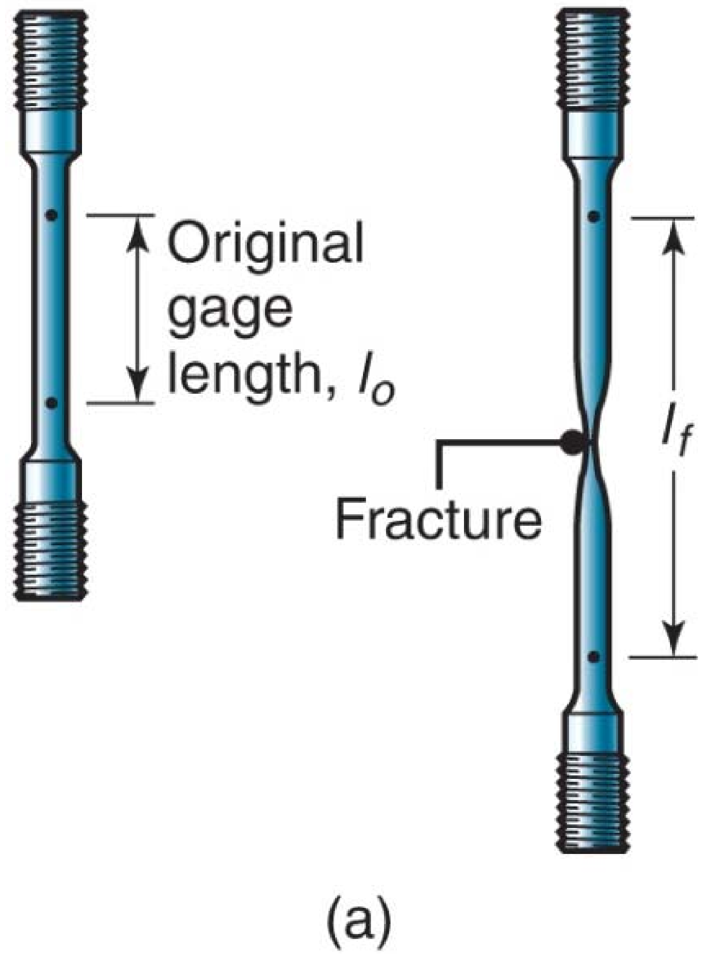

Figure 2.1 (2 of 2)

(b) Stages in specimen behavior in a tension test.

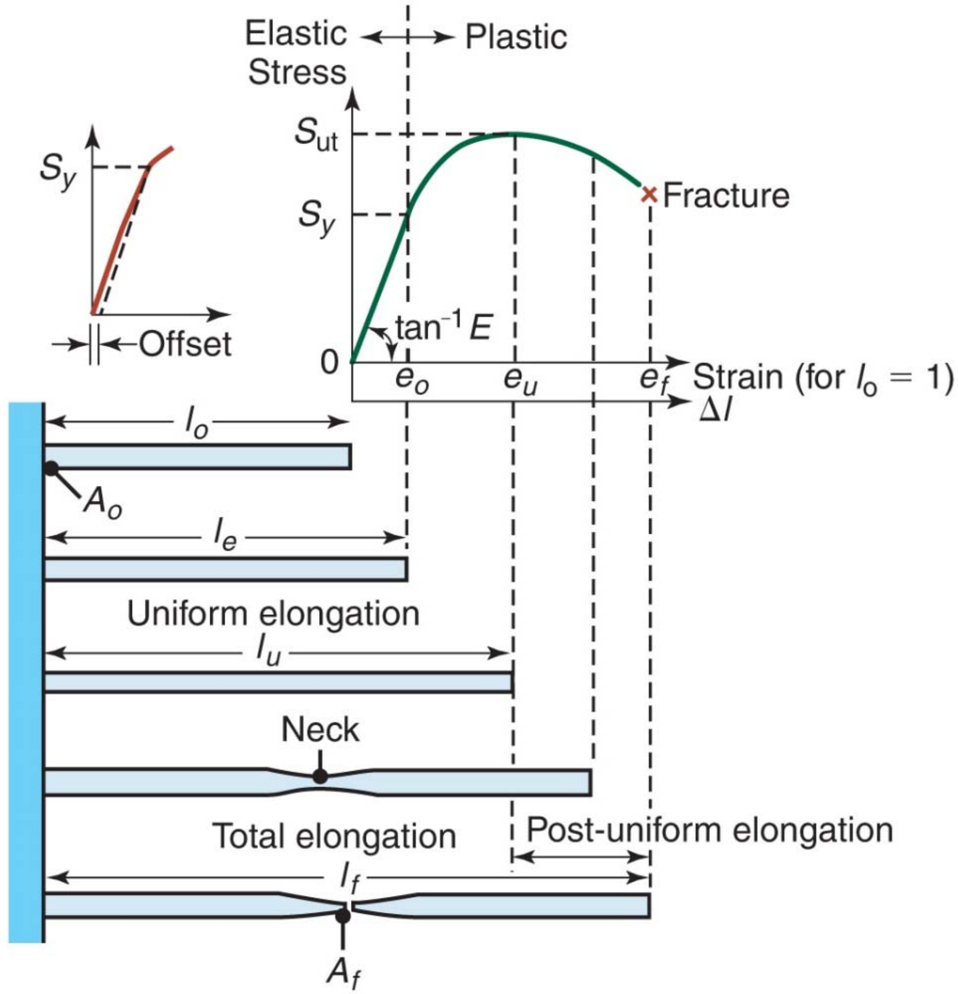

(b)

Figure 2.2

A typical stress–strain curve obtained from a tension test, showing various features.

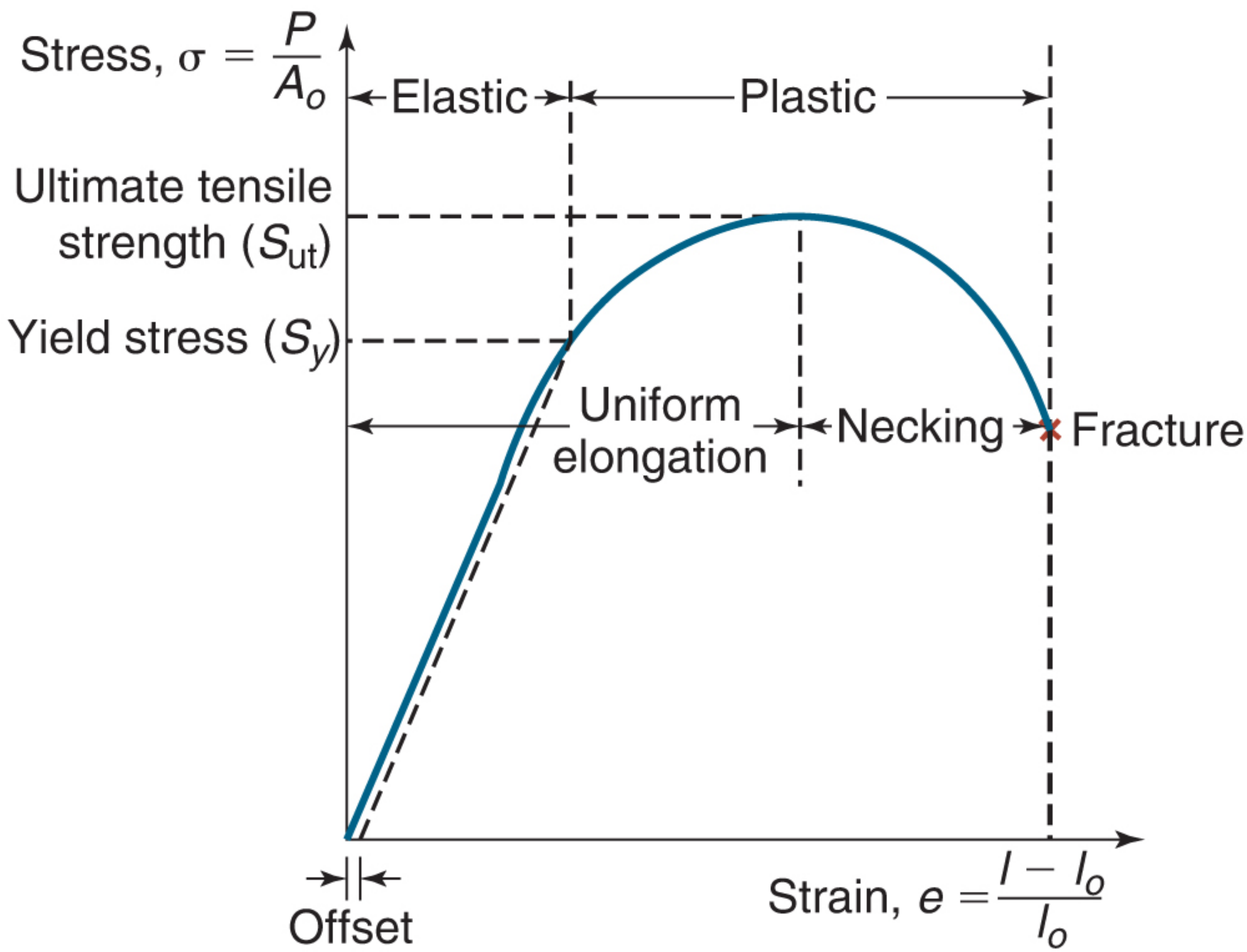

Pearson

Table 2.2 (1 of 2)

Mechanical Properties of Various Materials at Room Temperature.

Materials	Elastic modulus (GPa)	Yield strength (MPa)	Ultimate tensile strength (MPa)	Elongation in 50 mm (%)	Poisson's ratio, ν
Metals (wrought)					
Aluminum and its alloys	69–79	35–550	90–600	45–4	0.31–0.34
Copper and its alloys	105–150	76–110	140–1310	65–3	0.33–0.35
Lead and its alloys	14	14	20–55	50–9	0.43
Magnesium and its alloys	41–45	130–305	240–380	21–5	0.29–0.35
Molybdenum and its alloys	330–360	80–2070	90–2340	40–30	0.32
Nickel and its alloys	180–214	105–1200	345–1450	60–5	0.31
Steels	190–210	205–1725	415–1750	65–2	0.28–0.33
Titanium and its alloys	80–130	344–1380	415–1450	25–7	0.31–0.34
Tungsten and its alloys	350–400	550–690	620–760	0	0.27
Zinc and its alloys	50	25–180	240–550	65–5	0.27

Table 2.2 (2 of 2)

Mechanical Properties of Various Materials at Room Temperature.

Nonmetallic materials					
Ceramics	70–1000	—	140–2600	0	0.2
Diamond	820–1050	—	60,000	—	0.2
Glass and porcelain	70–80	—	140	0	0.24
Silicon carbide (SiC)	200–500	—	310–400	—	0.19
Silicon nitride (Si_2N_4)	280–310	—	160–580	—	0.26
Rubbers	0.01–0.1	—	—	—	0.5
Thermoplastics	1.4–3.4	—	7–80	1000–5	0.32–0.40
Thermoplastics, reinforced	2–50	—	20–120	10–1	0–0.5
Thermosets	3.5–17	—	35–170	0	0.34–0.5
Boron fibers	380	—	3500	0	0.27
Carbon fibers	275–415	—	2000–3000	0	0.21–0.28
Glass fibers	73–85	—	3500–4600	0	0.22–0.26
Kevlar fibers	62–117	—	2800	0	0.36
Spectra Fibers	73–100	—	2400–2800	3	0.46

Note: In the upper part of the table, the lowest values for E, S_y, and S_{ut} and the highest values for elongation are for pure metals. Multiply gigapascals (GPa) by 145,000 to obtain pounds per square in. (psi), megapascals (MPa) by 145 to obtain psi.

Figure 2.3

Schematic illustration of the loading and the unloading of a tensile-test specimen. Note that, during unloading, the curve follows a path parallel to the original elastic slope.

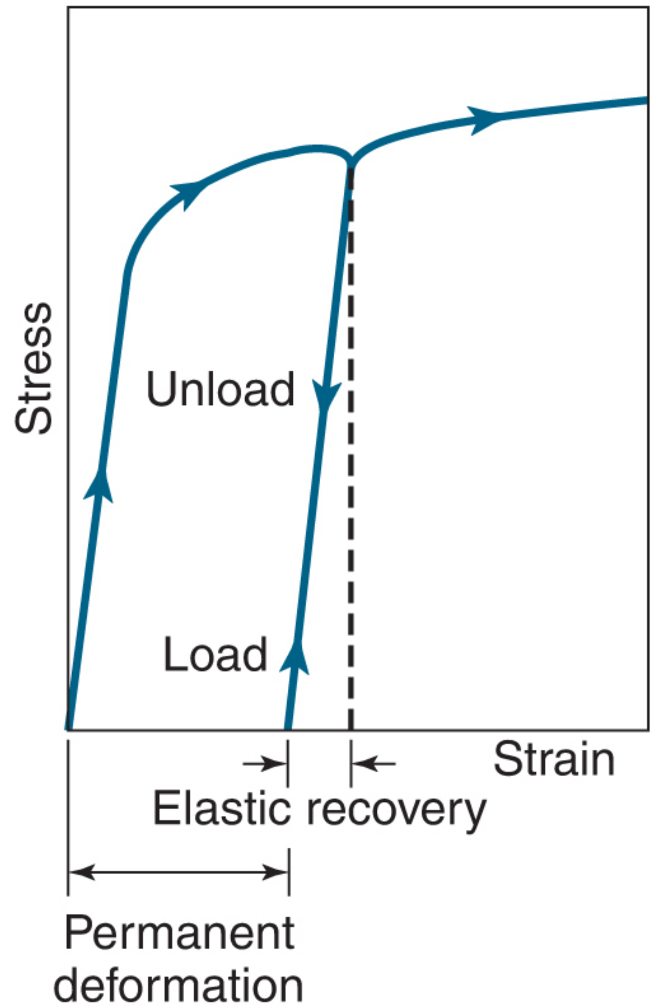

Figure 2.4 (1 of 4)

(a) Load–elongation curve in tension testing of a stainless steel specimen.

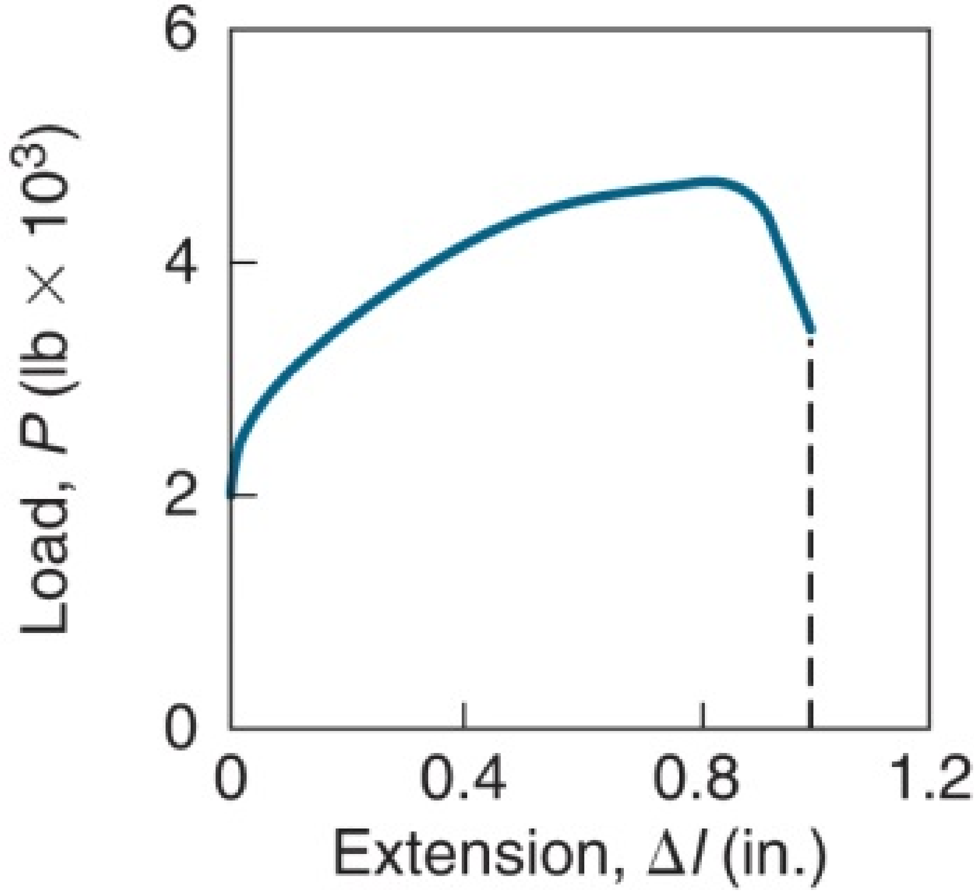

(a)

Figure 2.4 (2 of 4)

(b) Engineering stress–engineering strain curve, drawn from the data in Fig. 2.4a.

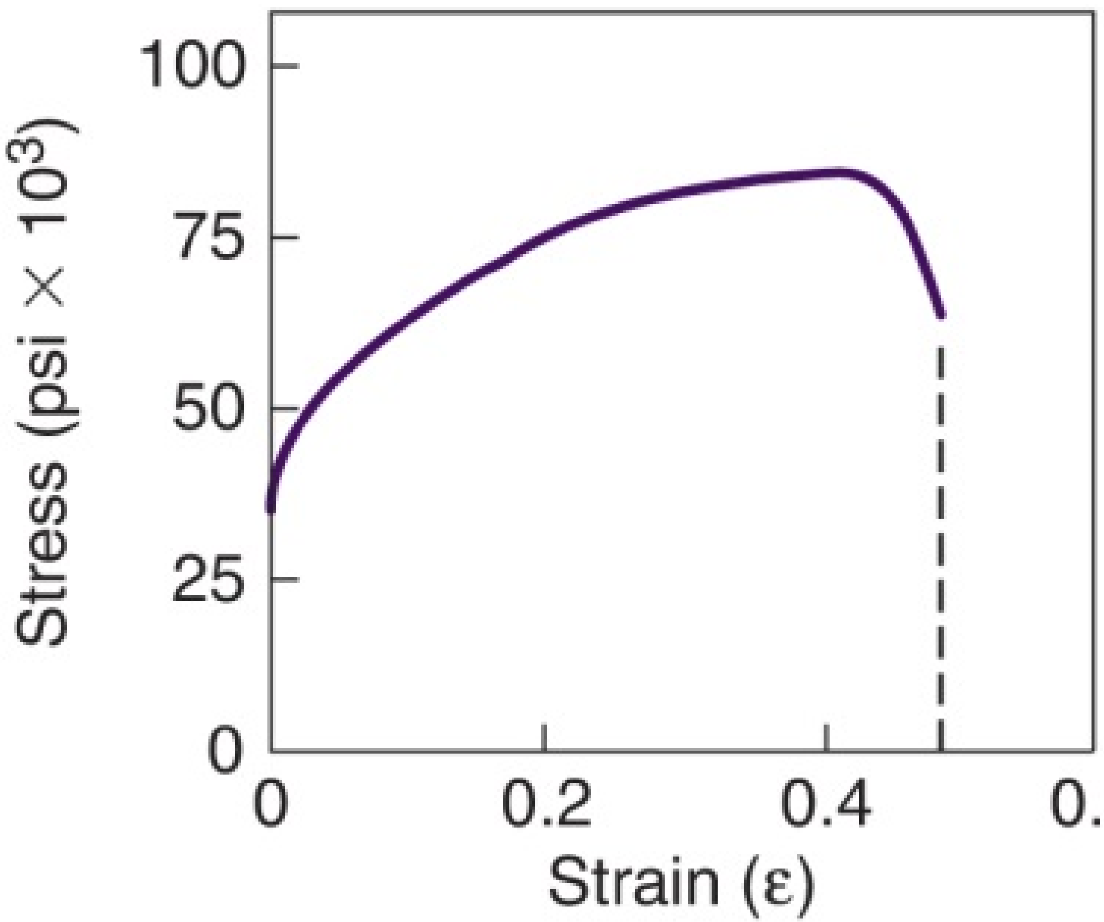

(b)

Figure 2.4 (3 of 4)

(c) True stress–true strain curve, drawn from the data in Fig. 2.4b. Note that this curve has a positive slope, indicating that the material is becoming stronger as it is strained.

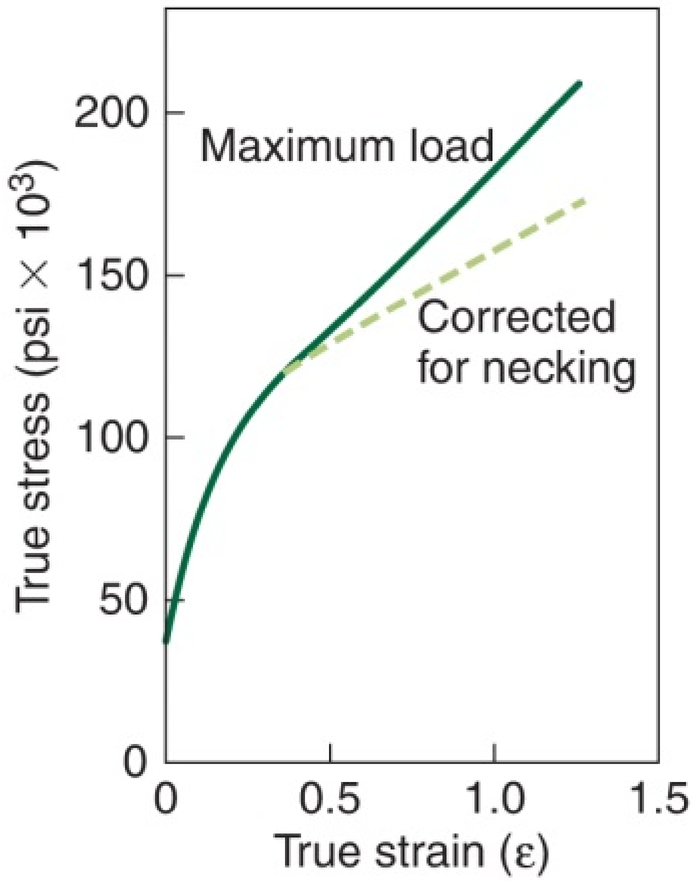

(c)

Figure 2.4 (4 of 4)

(d) True stress–true strain curve plotted on log–log paper and based on the corrected curve in Fig. 2.4c. The correction is due to the triaxial state of stress that exists in the necked region of the specimen.

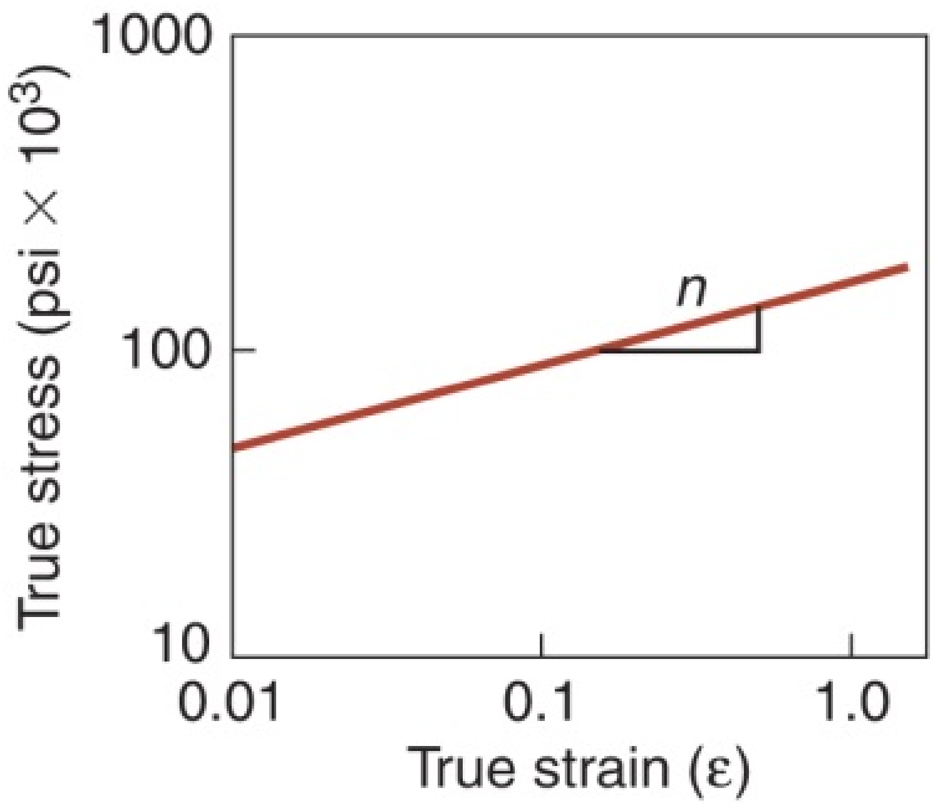

(d)

Pearson

Table 2.3 (1 of 2)

Typical Values for *K* and *n* for Selected Metals.

Material	*K* (MPa)	*n*
Aluminum		
1100–O	180	0.20
2024–T4	690	0.16
5052-O	202	0.13
6061–O	205	0.20
6061–T6	410	0.05
7075–O	400	0.17
Brass		
70–30, annealed	900	0.49
85–15, cold-rolled	580	0.34
Cobalt-base alloy, heat-treated	2070	0.50
Copper, annealed	315	0.54

Table 2.3 (2 of 2)

Typical Values for *K* and *n* for Selected Metals.

Steel		
Low-C, annealed	530	0.26
1020, annealed	745	0.20
4135, annealed	1015	0.17
4135, cold-rolled	1100	0.14
4340, annealed	640	0.15
304 stainless, annealed	1275	0.45
410 stainless, annealed	960	0.10
Titanium		
Ti-6Al-4V, annealed, 20°C	1400	0.015
Ti-6Al-4V, annealed, 200°C	1040	0.026
Ti-6Al-4V, annealed, 600°C	650	0.064
Ti-6Al-4V, annealed, 800°C	350	0.146

Figure 2.5

True stress–true strain curves in tension at room temperature for various metals. The curves start at a finite level of stress: The elastic regions have too steep a slope to be shown in this figure; thus, each curve starts at the yield strength, S_y, of the material.

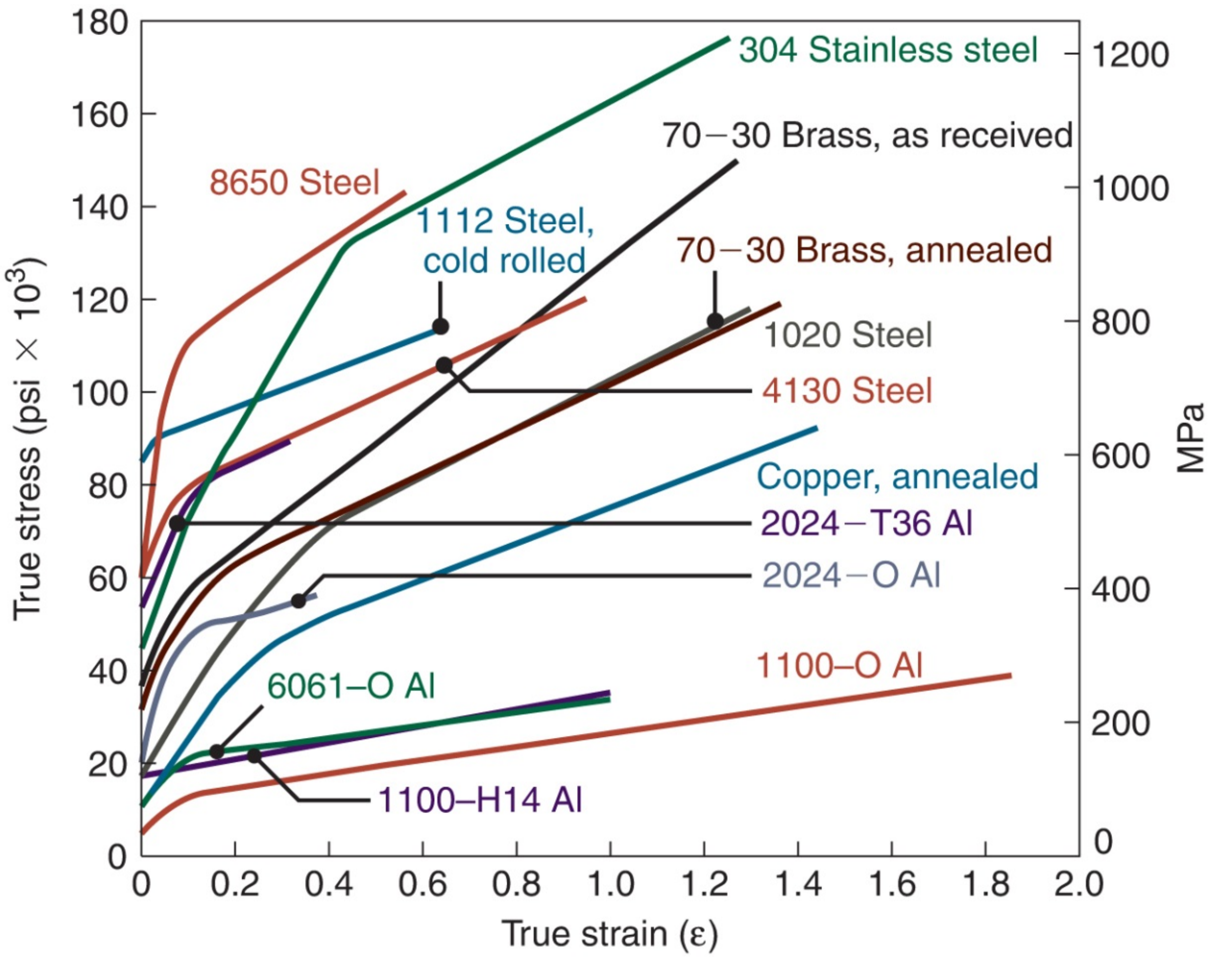

Figure 2.6

Effect of temperature on mechanical properties of carbon steel. Most materials display a similar temperature sensitivity for elastic modulus, yield strength, ultimate strength, and ductility.

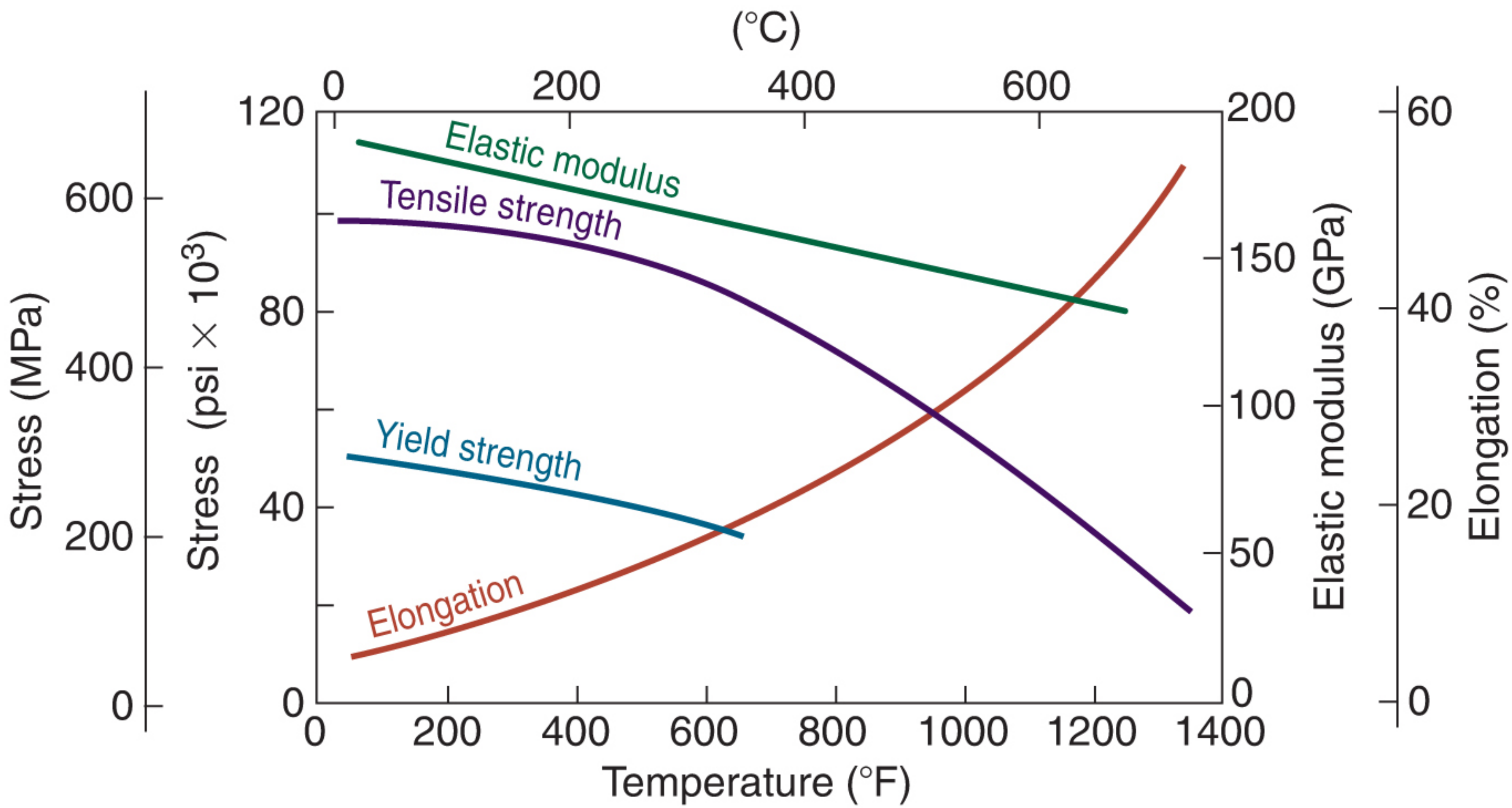

Table 2.4

Typical Ranges of Strain and Deformation Rate in Manufacturing Processes.

Process	True Strain	Deformation rate (m/s)
Cold working		
Forging, rolling	0.1–0.5	0.1–100
Wire and tube drawing	0.05–0.5	0.1–100
Explosive forming	0.05–0.2	10–100
Hot working and warm working		
Forging, rolling	0.1–0.5	0.1–30
Extrusion	2–5	0.1–1
Machining	1–10	0.1–100
Sheet-metal forming	0.1–0.5	0.05–2
Superplastic forming	0.2–3	10^{-4}–10^{-2}

Figure 2.7

The effect of strain rate on the ultimate tensile strength for aluminum. Note that, as the temperature increases, the slopes of the curves increase; thus, strength becomes more and more sensitive to strain rate as temperature increases.

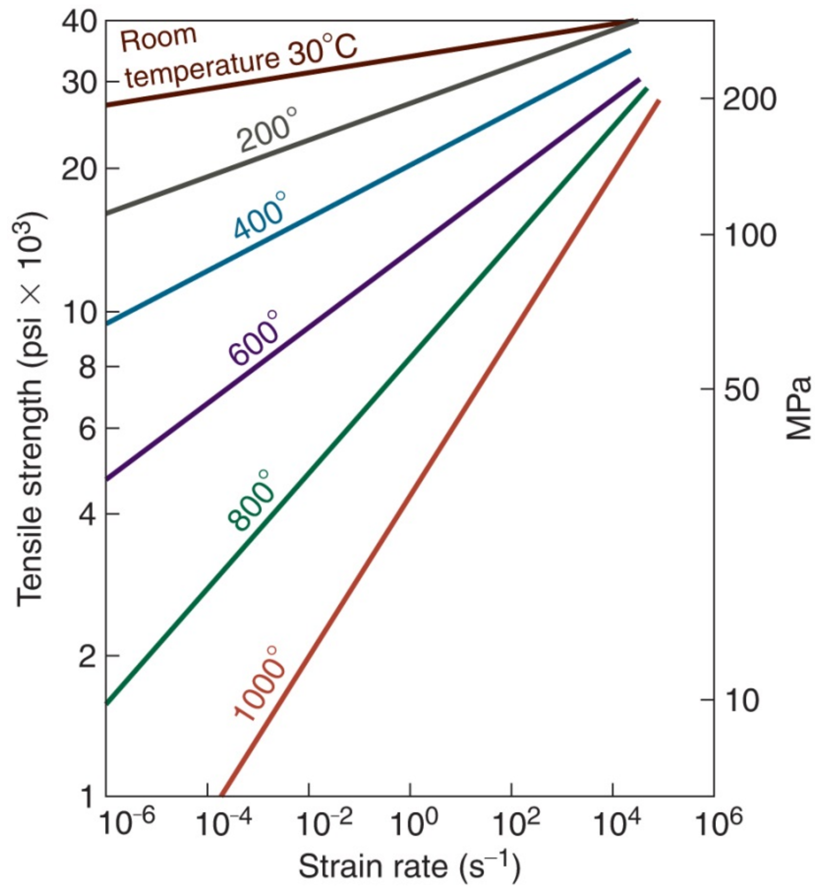

Source: J.H. Hollomon.

Figure 2.8

Barreling in compressing a round solid cylindrical specimen (7075-O aluminum) between flat dies. Barreling is caused by friction at the die–specimen interfaces, which retards the free flow of the material (see also Fig. 14.3).

Figure 2.9

Disk test on a brittle material, showing the direction of loading and the fracture path.

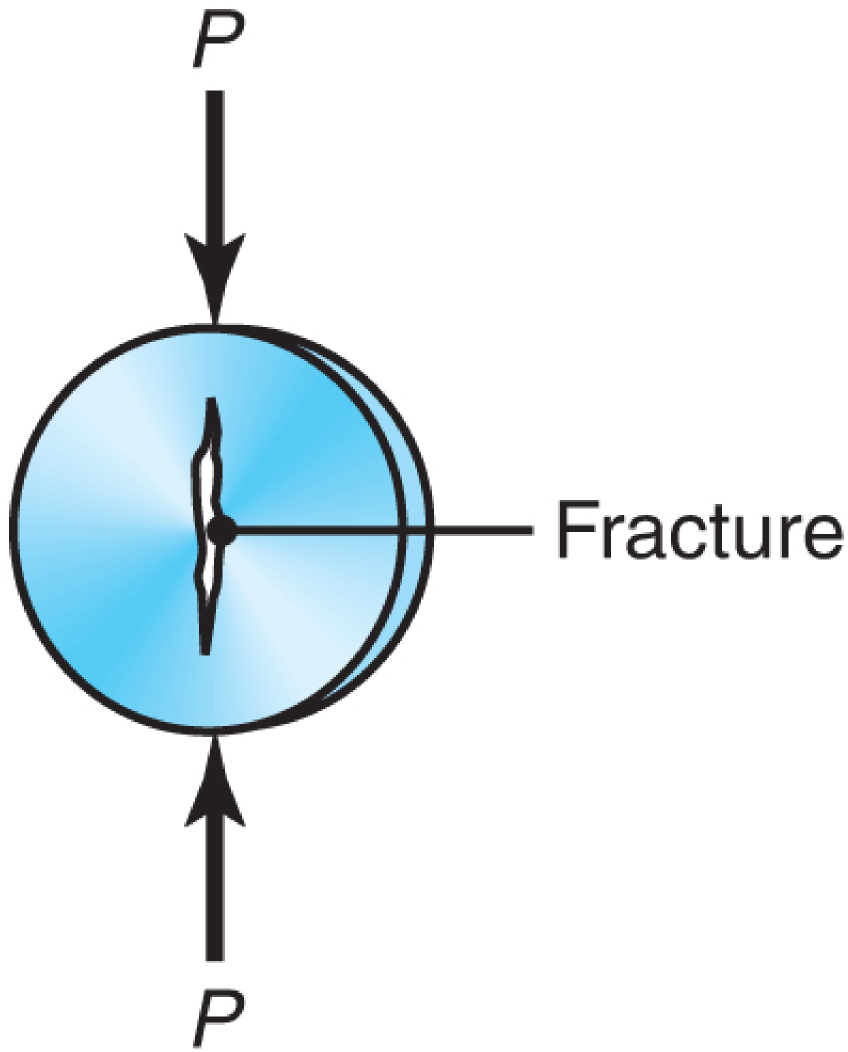

Figure 2.10

A typical torsion-test specimen, mounted between the two heads of a testing machine and twisted. Note the shear deformation of an element in the reduced section of the specimen.

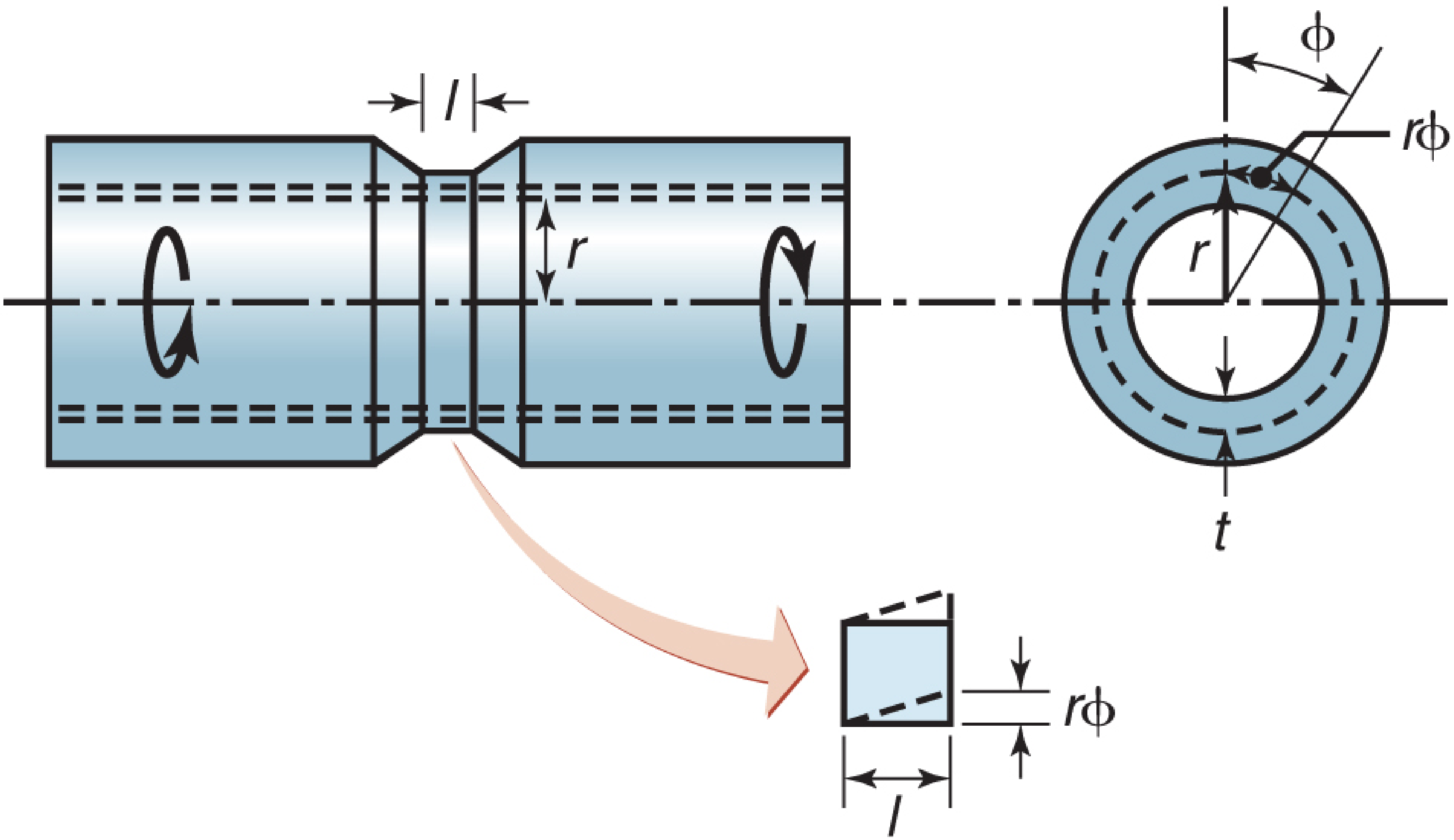

Figure 2.11

Two bend-test methods for brittle materials: (a) three-point bending, and (b) four-point bending. The two areas shown above the beams represent the bending-moment diagrams, described in texts on the mechanics of solids. Note the region of constant maximum bending moment in (b); by contrast, the maximum bending moment occurs only at the center of the specimen in (a).

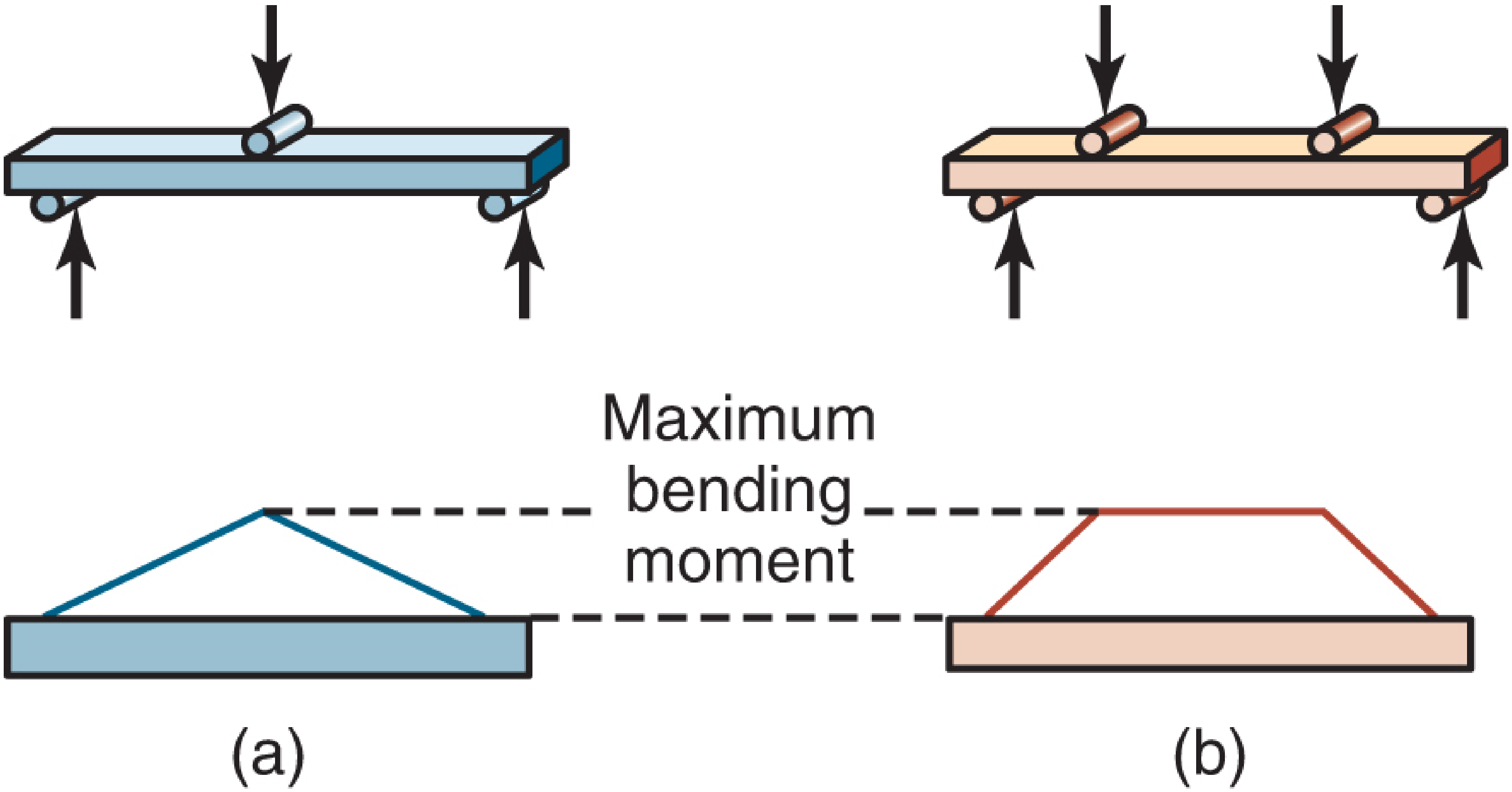

Pearson

Figure 2.12 (1 of 3)

A selection of hardness testers. (a) A Micro Vickers hardness tester.

(a)

Figure 2.12 (2 of 3)

A selection of hardness testers. (b) Rockwell hardness tester.

(b)

Figure 2.12 (3 of 3)

A selection of hardness testers. (c) Leeb tester.

(c)

Source: (a) and (b) Courtesy of Buehler (c) Courtesy of Wilson® Instruments.

Figure 2.13

General characteristics of hardness-testing methods and formulas for calculating hardness.

Test	Indenter	Shape of indentation: Side view	Shape of indentation: Top view	Load, *P*	Hardness number
Brinell	10-mm steel or tungsten-carbide ball	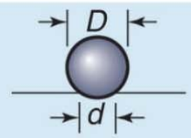 D, d	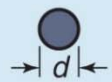 d	500 kg 1500 kg 3000 kg	$\text{HB} = \dfrac{2P}{(\pi D)\left(D - \sqrt{D^2 - d^2}\right)}$
Vickers	Diamond pyramid	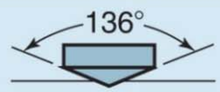 136°	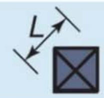 L	1–120 kg	$\text{HV} = \dfrac{1.854P}{L^2}$
Knoop	Diamond pyramid	 $L/b = 7.11$ $b/t = 4.00$ t	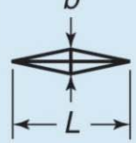 b, L	25 g–5 kg	$\text{HK} = \dfrac{14.2P}{L^2}$
Rockwell A C D	Diamond cone	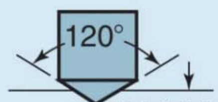 120° t = mm		60 kg 150 kg 100 kg	HRA HRC HRD $\}$ $= 100 - 500t$
B F G	$\frac{1}{16}$-in. diameter steel ball	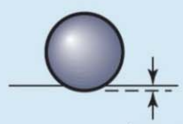 t = mm		100 kg 60 kg 150 kg	HRB HRF HRG $\}$ $= 130 - 500t$
E	$\frac{1}{8}$-in. diameter steel ball			100 kg	HRE $\}$ $= 130 - 500t$

Pearson

Figure 2.14

Indentation geometry in Brinell hardness testing: (a) annealed metal.

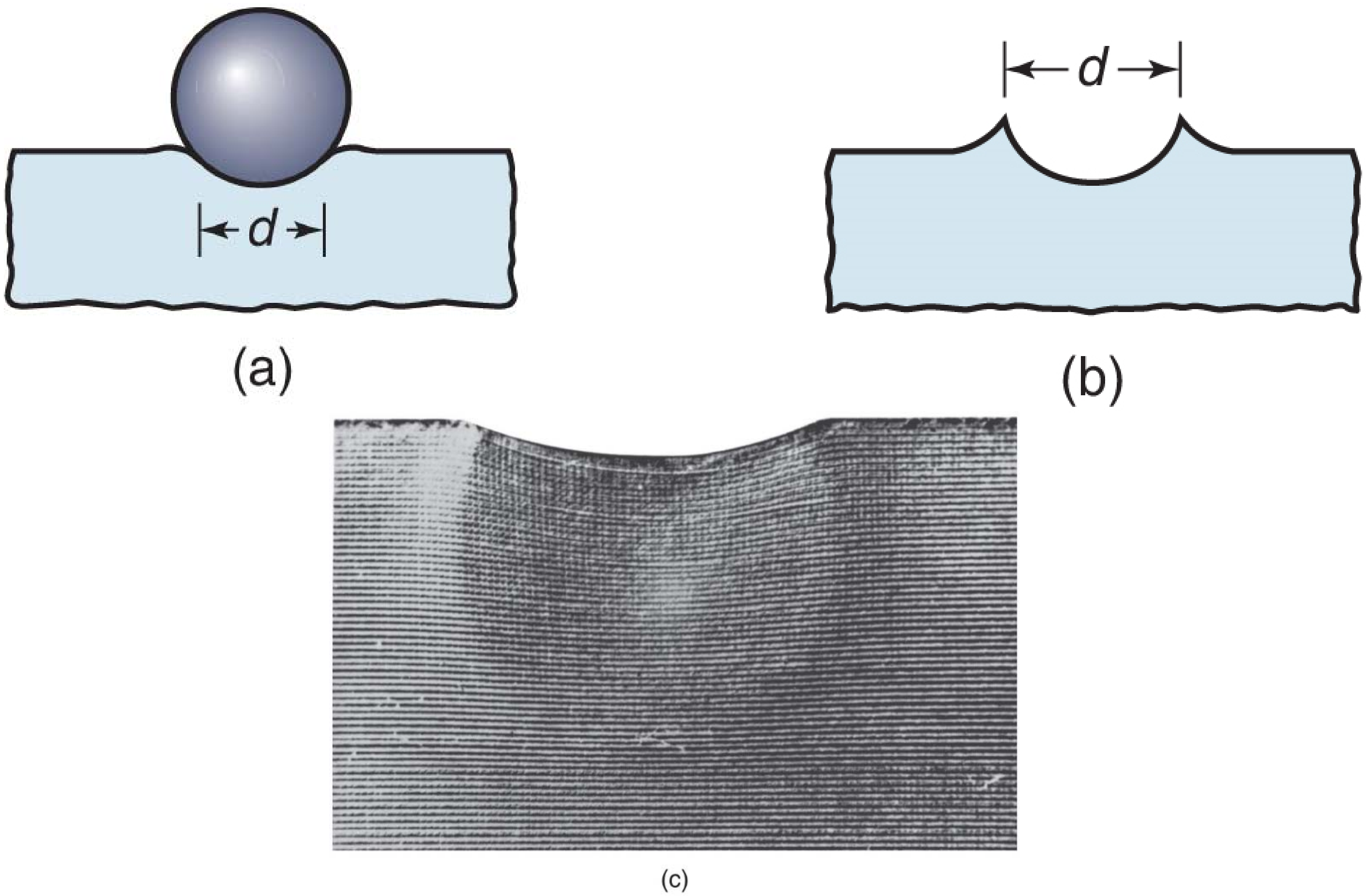

Pearson

Figure 2.15

Chart for converting various hardness scales; note the limited range of most of the scales. Because of the many factors involved, these conversions are approximate.

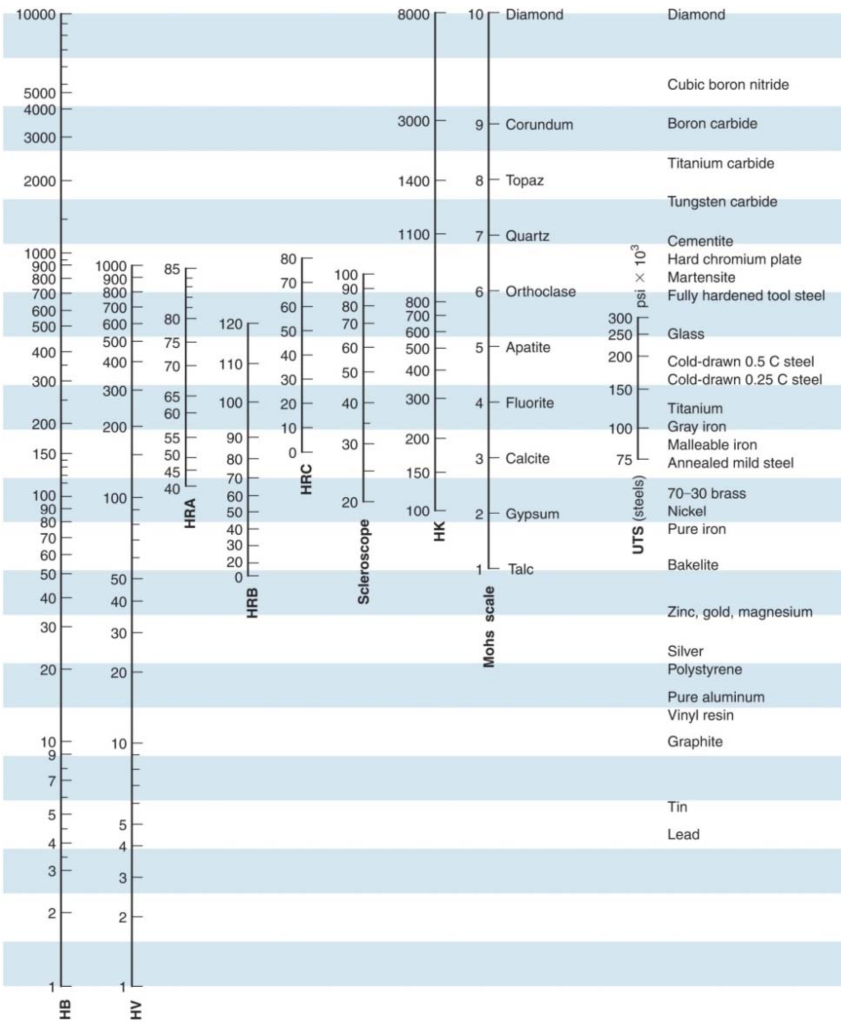

Figure 2.16 (1 of 2)

(a) Typical *S-N* curves for two metals. Note that, unlike steel, aluminum does not have an endurance limit.

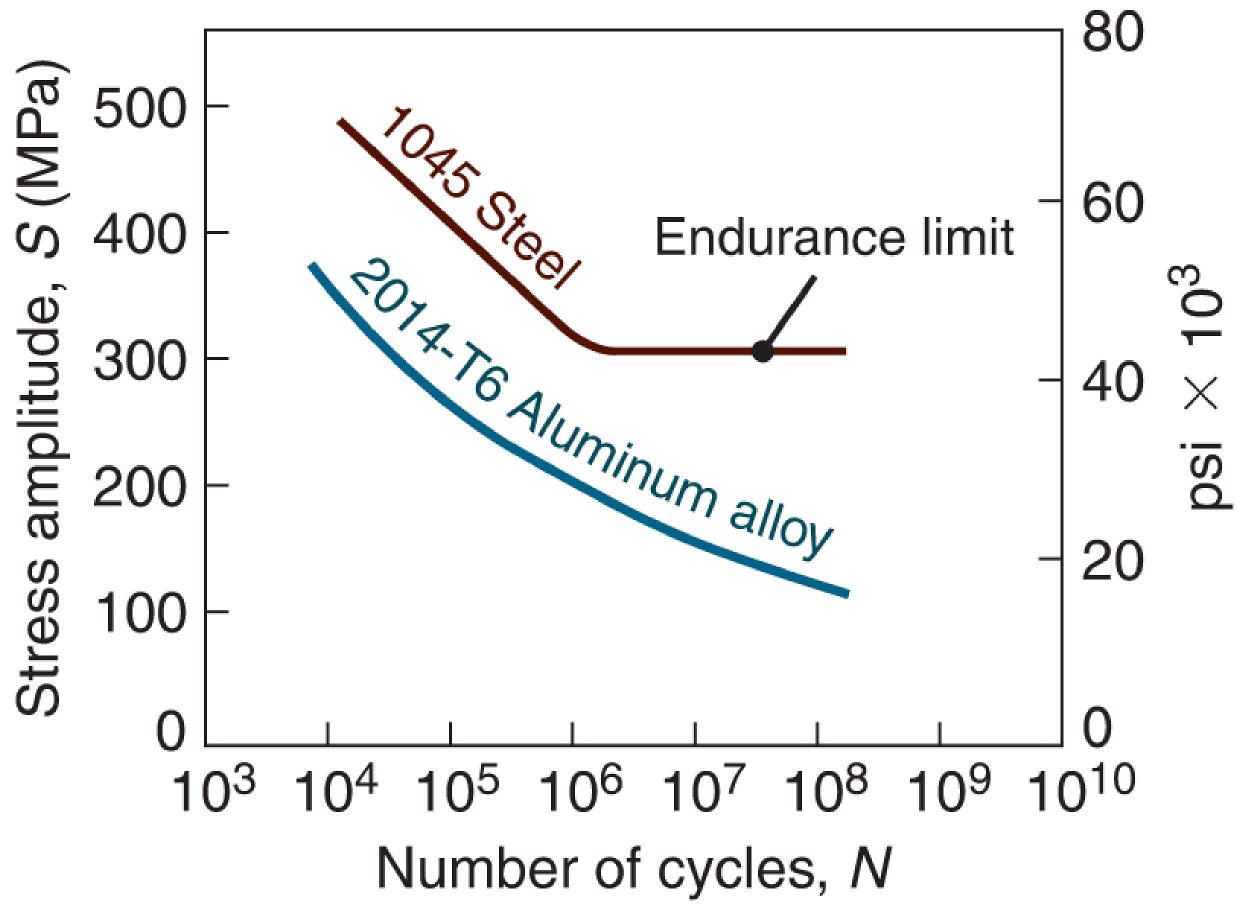

(a)

Figure 2.16 (2 of 2)

(b) *S-N* curves for common polymers.

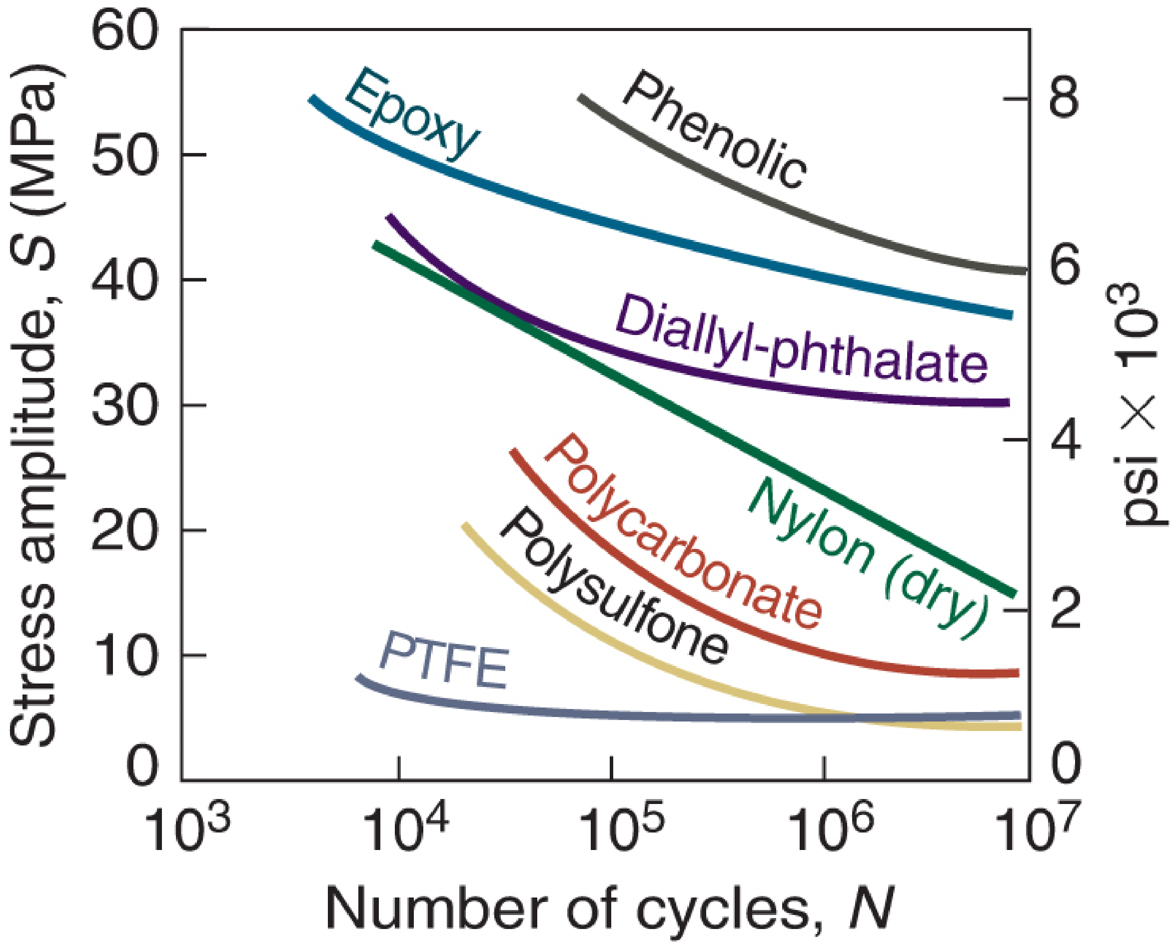

(b)

Figure 2.17

Ratio of endurance limit to tensile strength for various metals, as a function of tensile strength. Because aluminum does not have an endurance limit, the correlations for aluminum are based on a specific number of cycles, as is seen in Fig. 2.16.

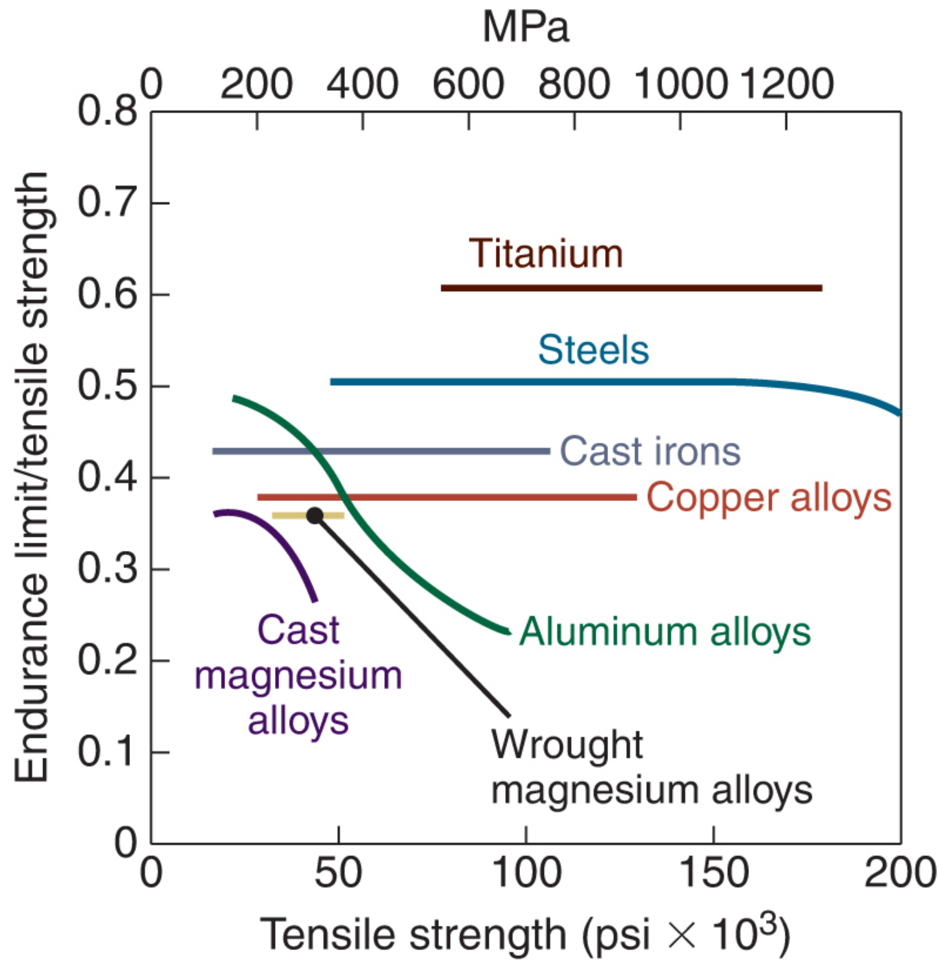

Figure 2.18

Schematic illustration of a typical creep curve. The linear segment of the curve (secondary) is used in designing components for a specific creep life.

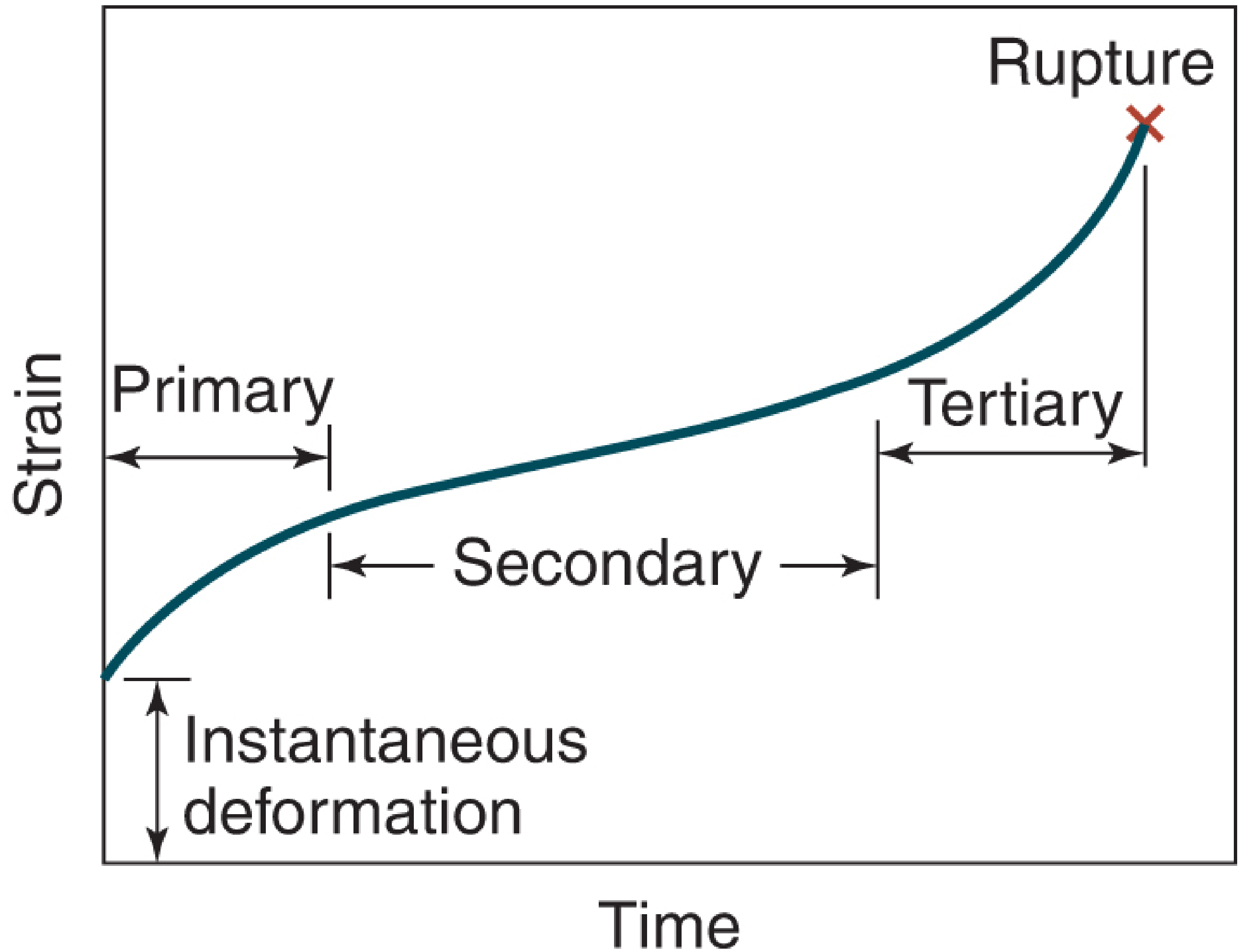

Figure 2.19 (1 of 2)

Impact test specimens. (a) Izod

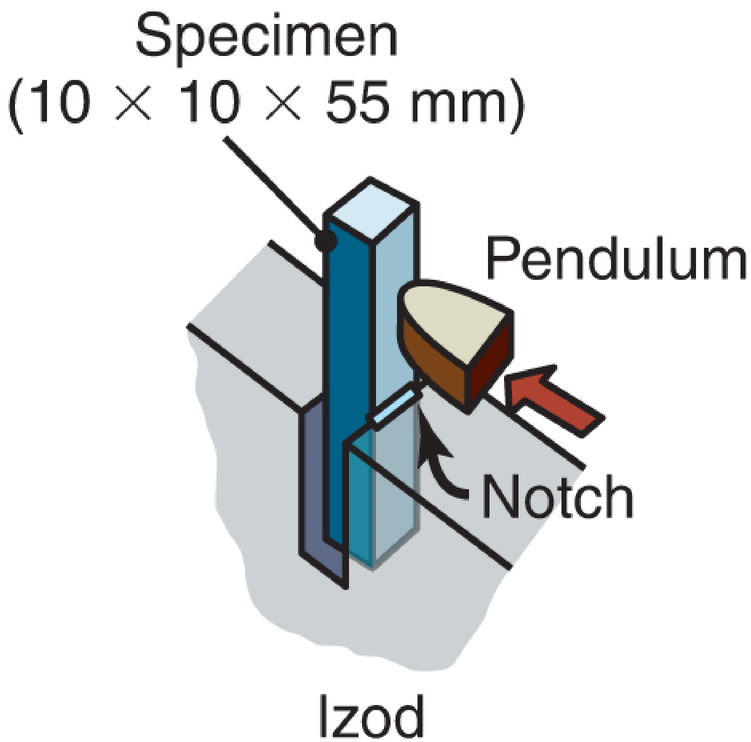

(a)

Pearson

Figure 2.19 (2 of 2)

Impact test specimens. (b) Charpy.

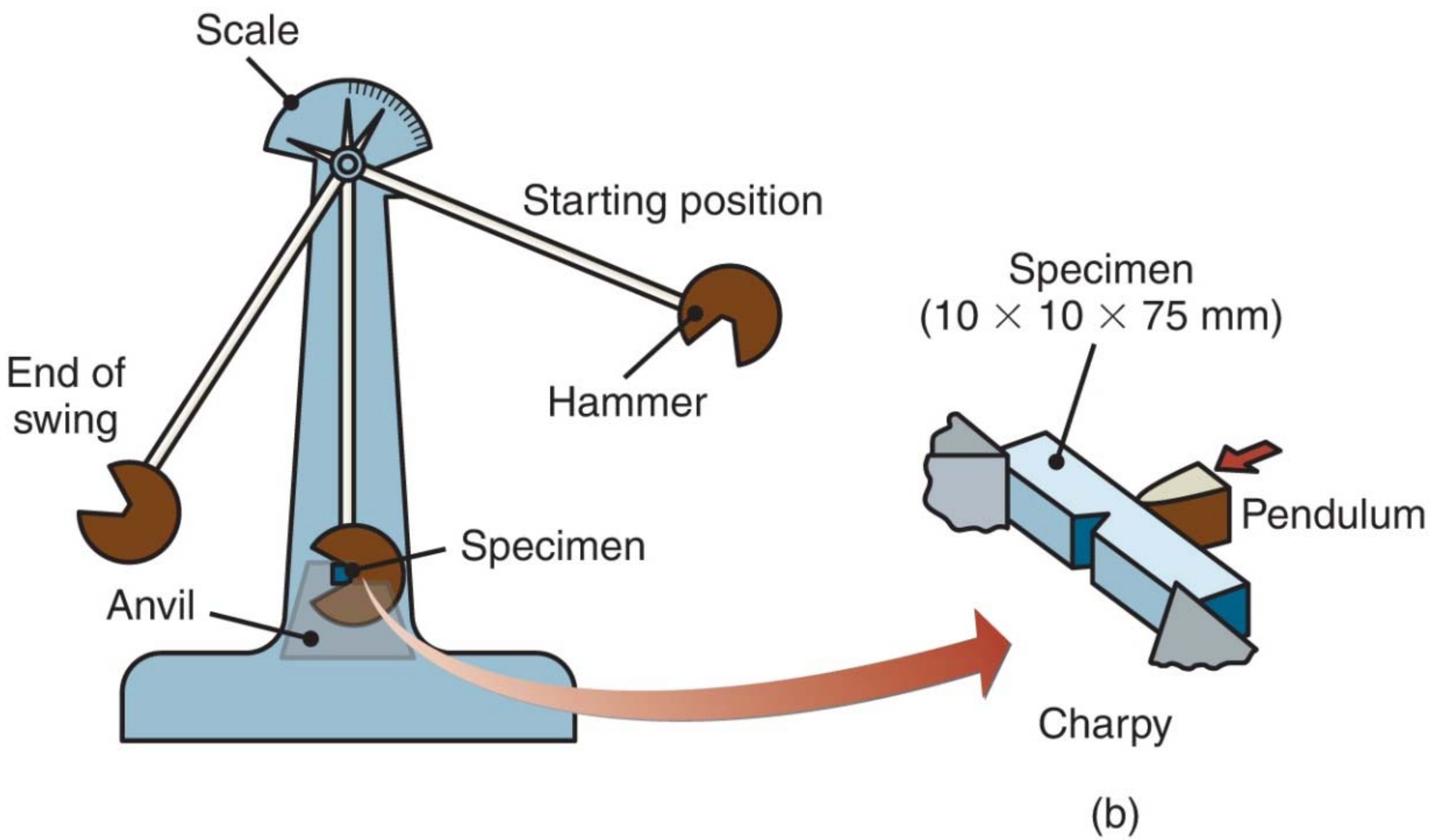

Figure 2.20 (1 of 4)

Schematic illustration of types of failures in materials: (a) necking and fracture of ductile materials.

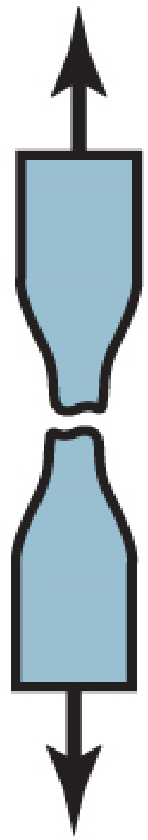

(a)

Pearson

Figure 2.20 (2 of 4)

Schematic illustration of types of failures in materials: (b) buckling of ductile materials under a compressive load.

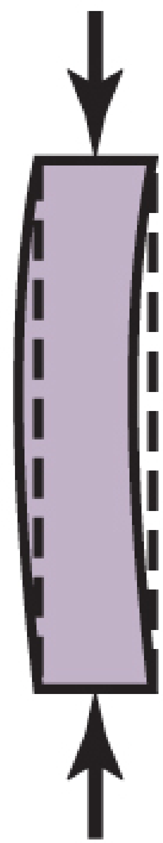

(b)

Figure 2.20 (3 of 4)

Schematic illustration of types of failures in materials: (c) fracture of brittle materials in compression.

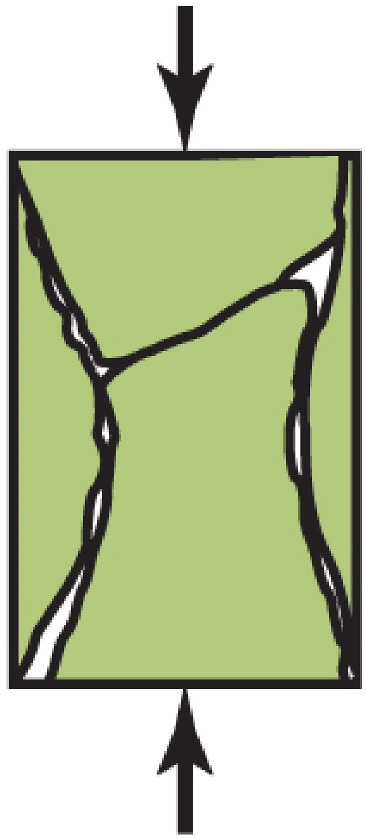

(c)

Figure 2.20 (4 of 4)

Schematic illustration of types of failures in materials: (d) cracking on the barreled surface of ductile materials in compression.

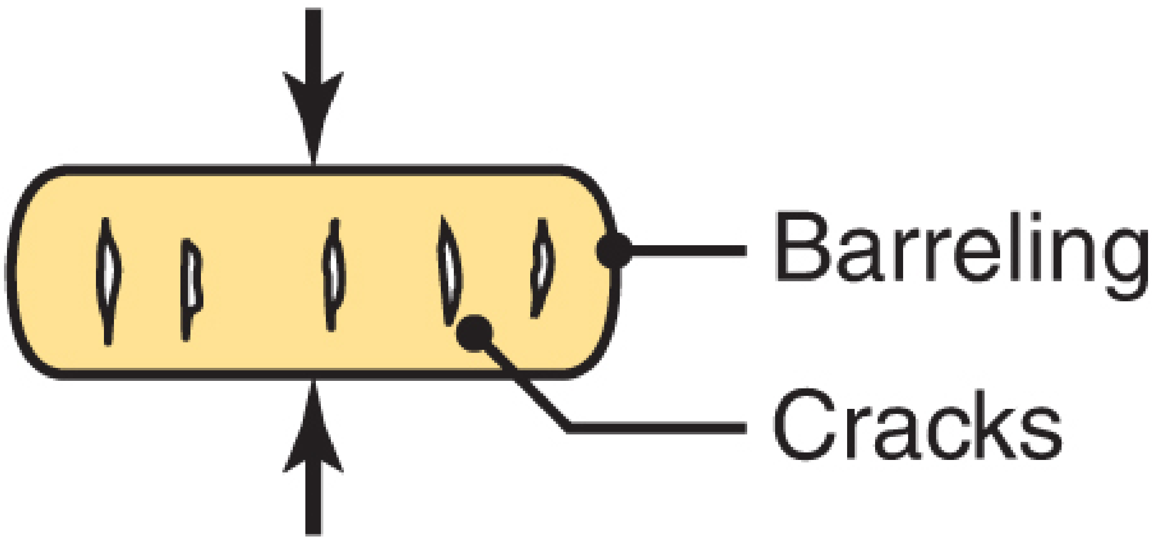

(d)

Figure 2.21 (1 of 4)

Schematic illustration of the types of fracture in tension: (a) brittle fracture in polycrystalline metals.

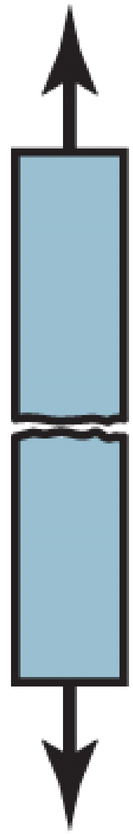

(a)

Figure 2.21 (2 of 4)

Schematic illustration of the types of fracture in tension: (b) shear fracture in ductile single crystals—see also Fig. 1.6a.

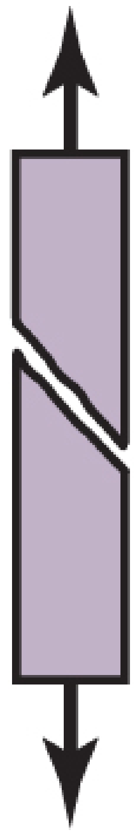

(b)

Figure 2.21 (3 of 4)

Schematic illustration of the types of fracture in tension: (c) ductile cup-and-cone fracture in polycrystalline metals.

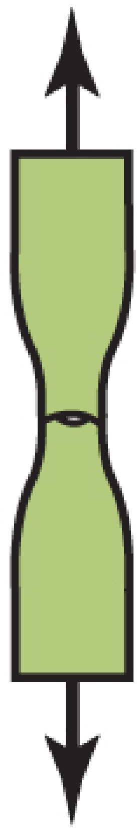

(c)

Figure 2.21 (4 of 4)

Schematic illustration of the types of fracture in tension: (d) complete ductile fracture in polycrystalline metals, with 100% reduction of area.

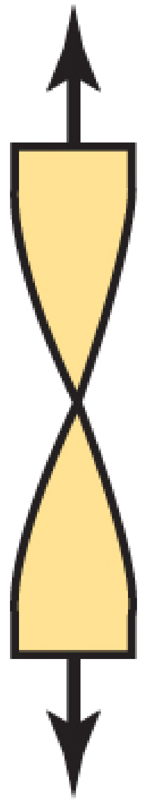

(d)

Figure 2.22

Surface of ductile fracture in low-carbon steel, showing dimples. Fracture is usually initiated at impurities, inclusions, or preexisting voids (microporosity) in the metal.

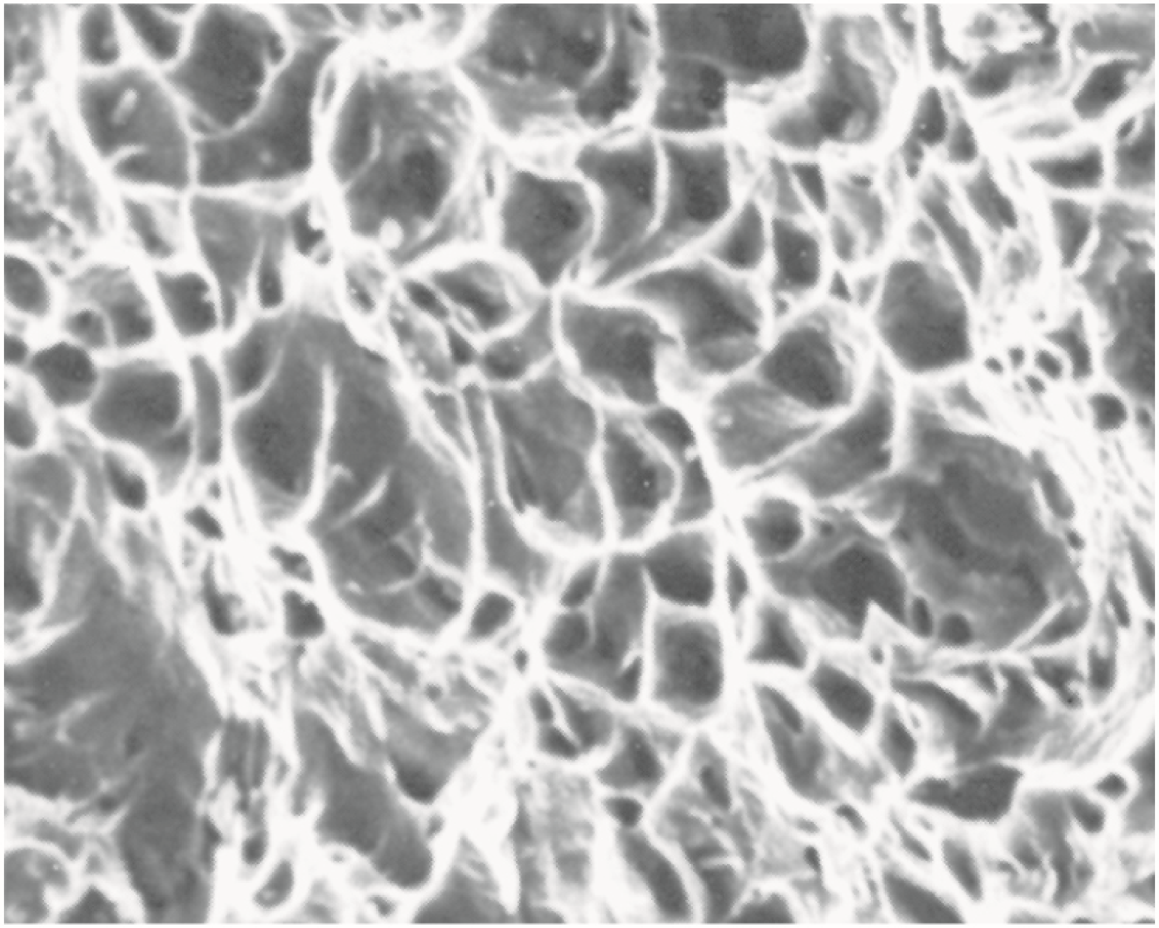

Source: After K.-H. Habig and D. Klaffke.

Figure 2.23 (1 of 5)

Sequence of events in the necking and fracture of a tensile-test specimen: (a) early stage of necking.

(a)

Figure 2.23 (2 of 5)

Sequence of events in the necking and fracture of a tensile-test specimen: (b) small voids begin to form within the necked region.

(b)

Figure 2.23 (3 of 5)

Sequence of events in the necking and fracture of a tensile-test specimen: (c) voids coalesce, producing an internal crack.

(c)

Figure 2.23 (4 of 5)

Sequence of events in the necking and fracture of a tensile-test specimen: (d) the rest of the cross section begins to fail at the periphery, by shearing.

(d)

Figure 2.23 (5 of 5)

Sequence of events in the necking and fracture of a tensile-test specimen: (e) the final fracture, known as a cup- (top fracture surface) and-cone- (bottom surface) fracture, surfaces.

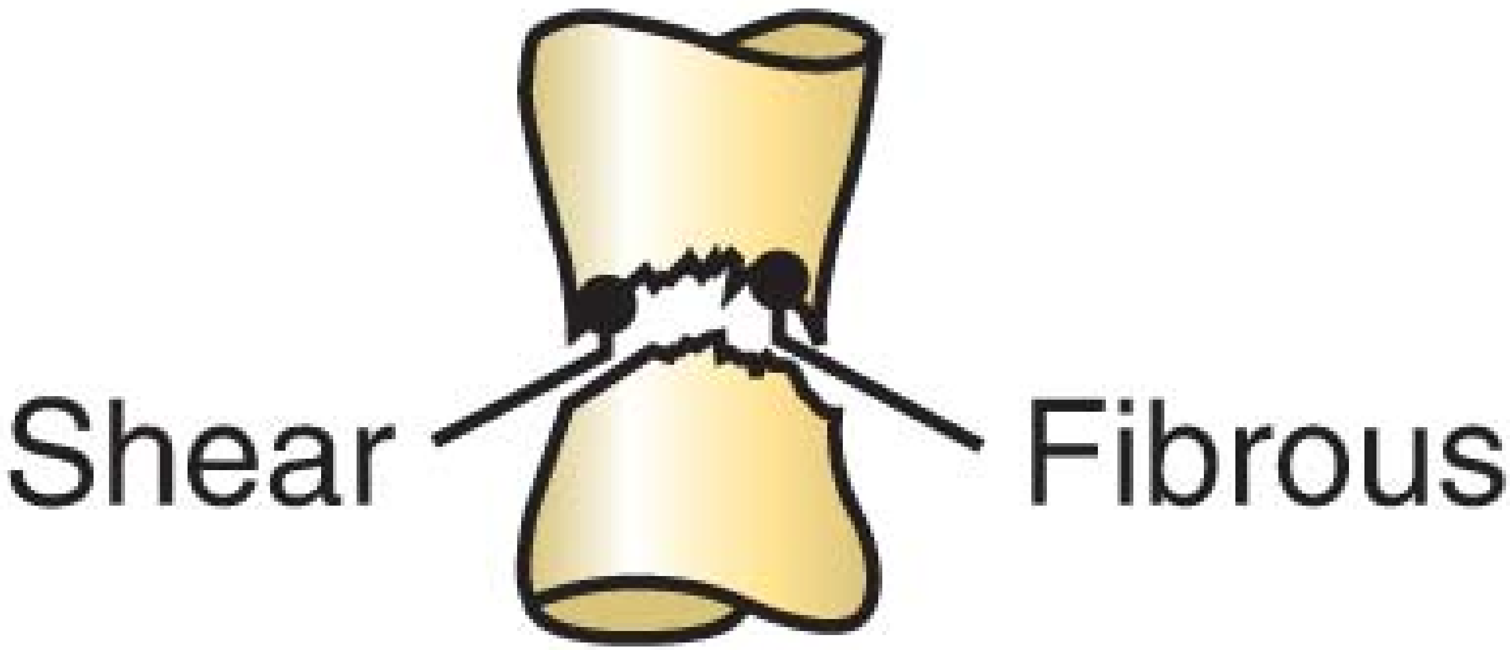

(e)

Pearson

Figure 2.24

Schematic illustration of the deformation of soft and hard inclusions and of their effect on void formation in plastic deformation. Note that, because they do not conform to the overall deformation of the ductile matrix, hard inclusions can cause internal voids.

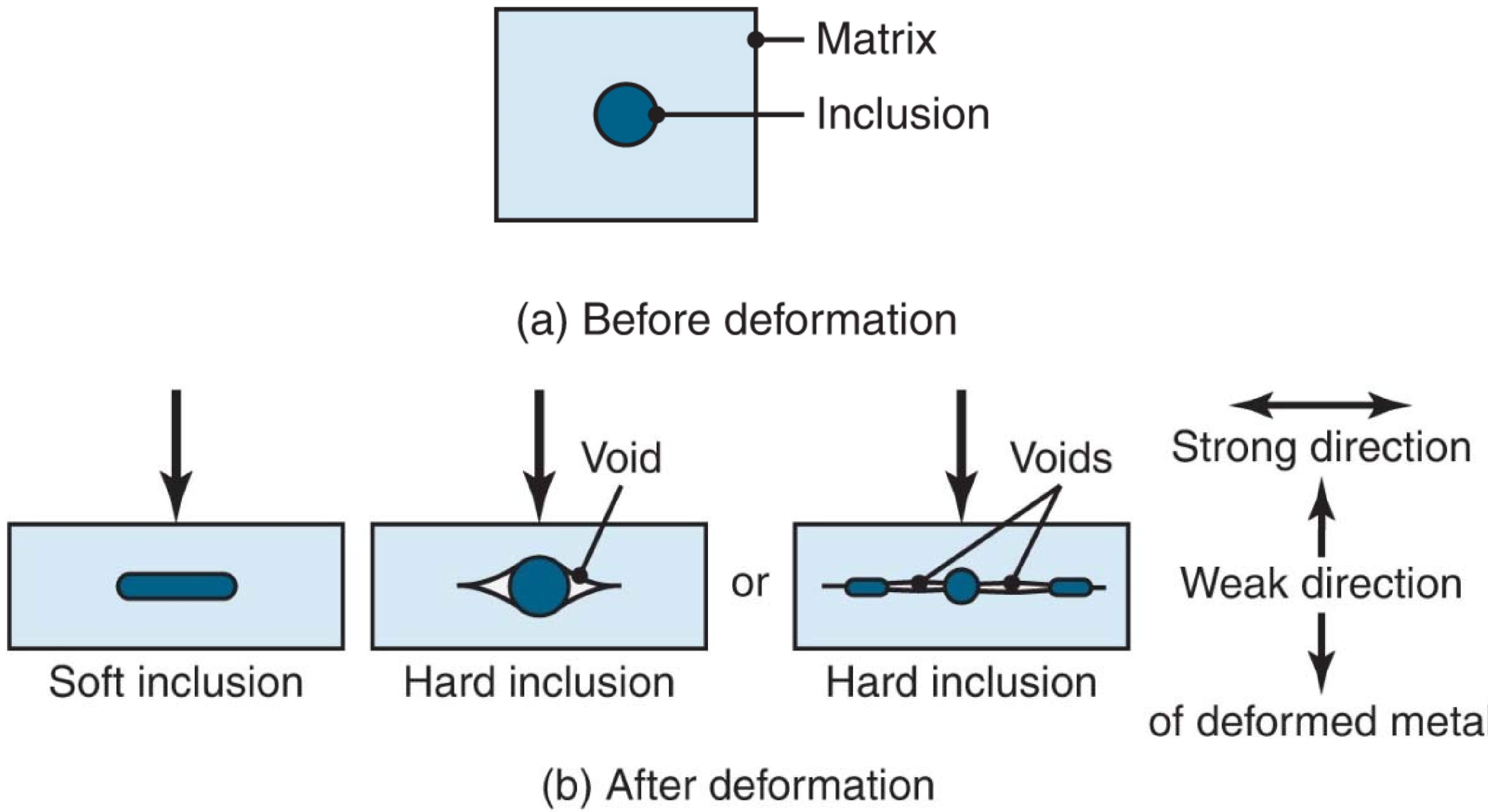

Figure 2.25

Schematic illustration of transition temperature in metals.

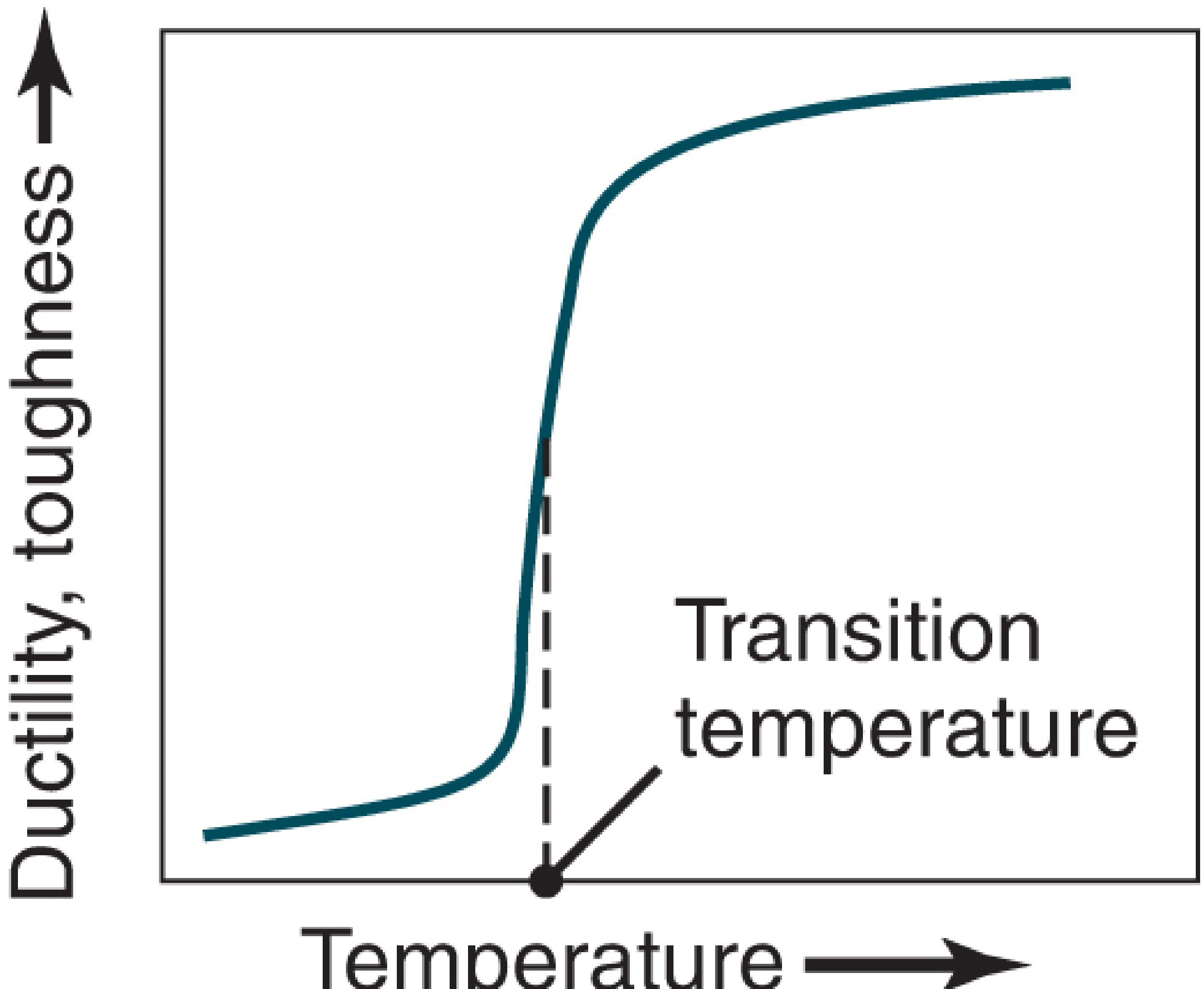

Figure 2.26

Fracture surface of steel that has failed in a brittle manner. The fracture path is transgranular (through the grains). Magnification: 200×.

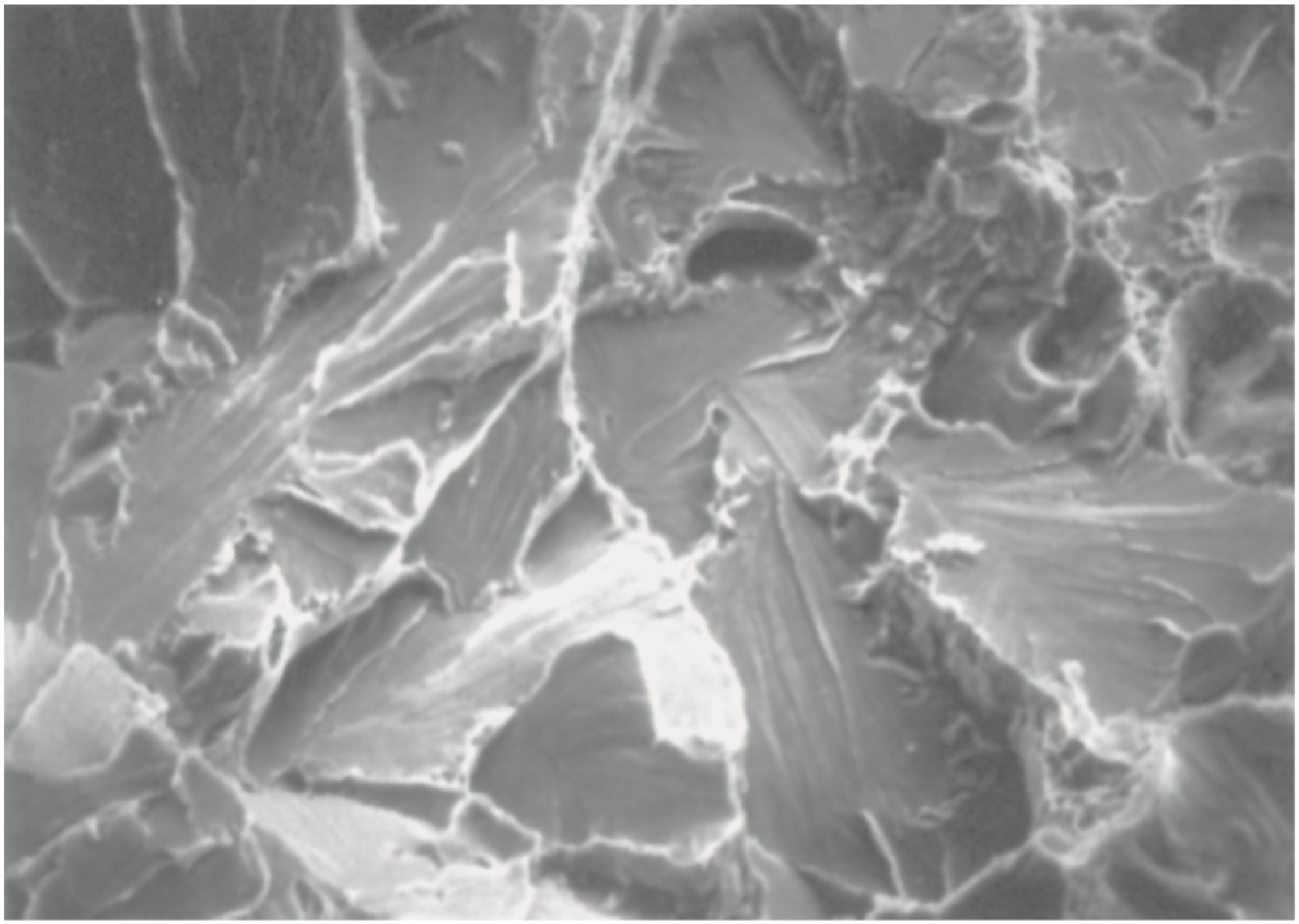

Source: After B.J. Schulze and S.L. Meiley and Packer Engineering Associates, Inc.

Figure 2.27

Intergranular fracture, at two different magnifications. Grains and grain boundaries are clearly visible in this micrograph. The fracture path is along the grain boundaries. Magnification: left, 100×; right, 500×.

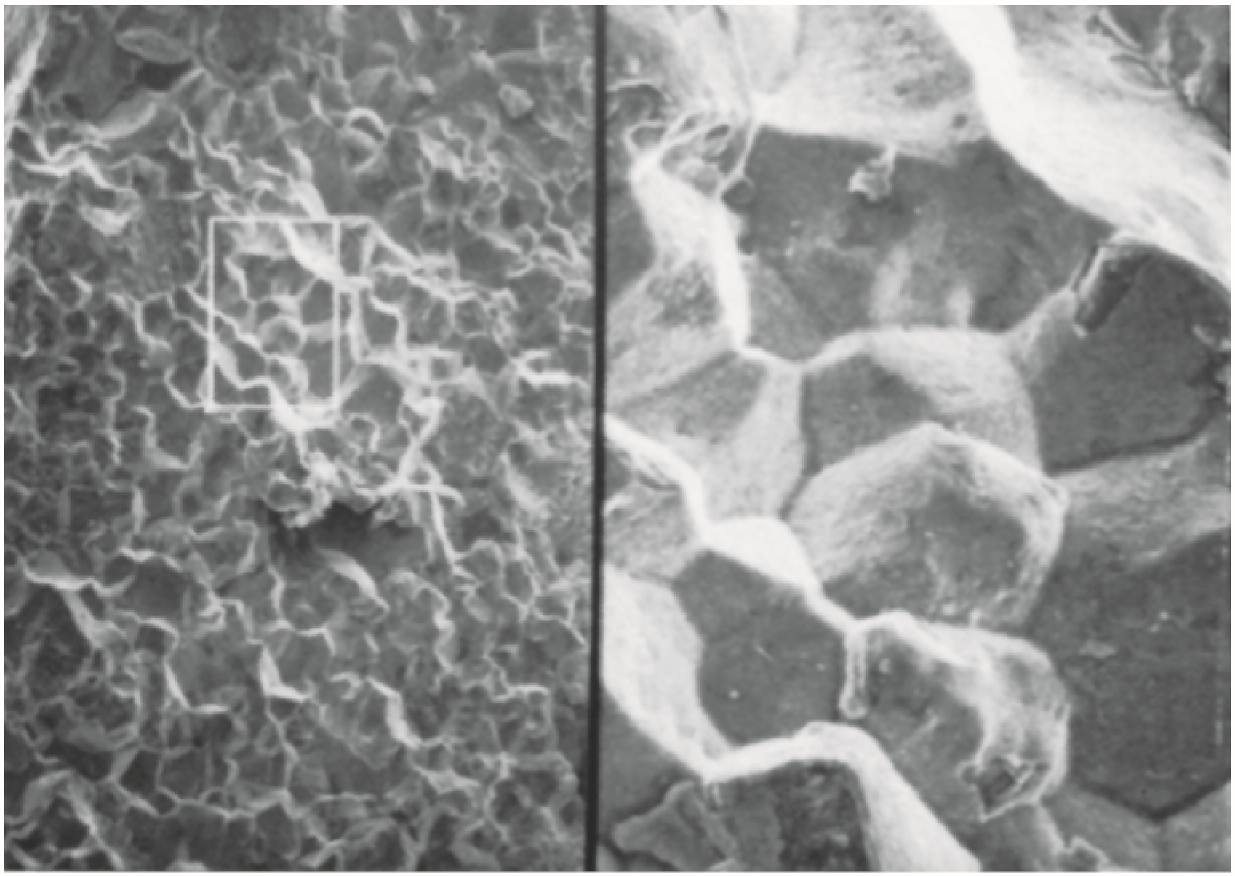

Source: After B.J. Schulze and S.L. Meiley and Packer Engineering Associates, Inc.

Figure 2.28

Typical fatigue-fracture surface on metals, showing beach marks. Magnification: left, 500×; right, 1000×.

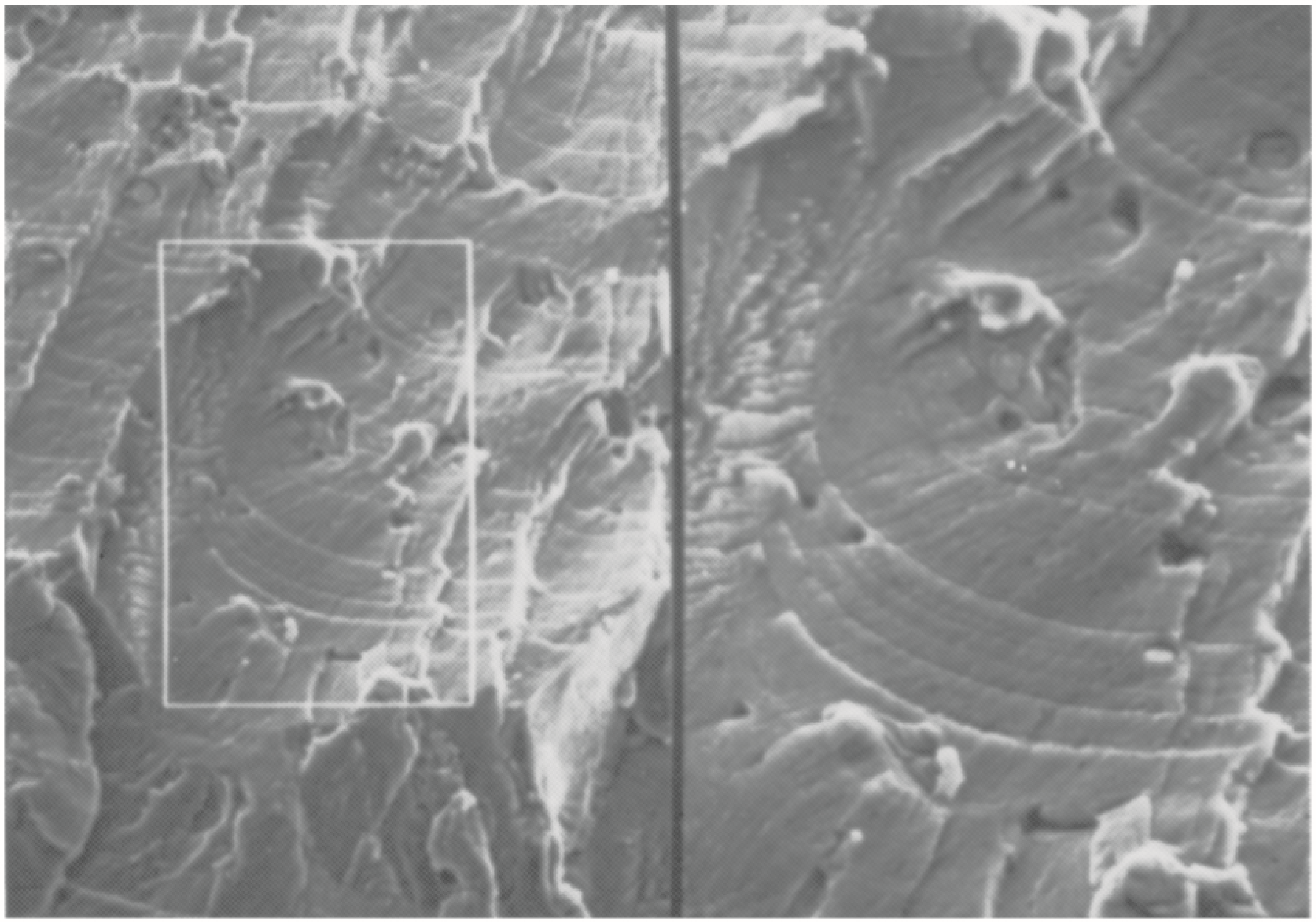

Source: After B.J. Schulze and S.L. Meiley and Packer Engineering Associates, Inc.

Figure 2.29

Reductions in the fatigue strength of cast steels subjected to various surface-finishing operations. Note that the reduction becomes greater as the surface roughness and the strength of the steel increase.

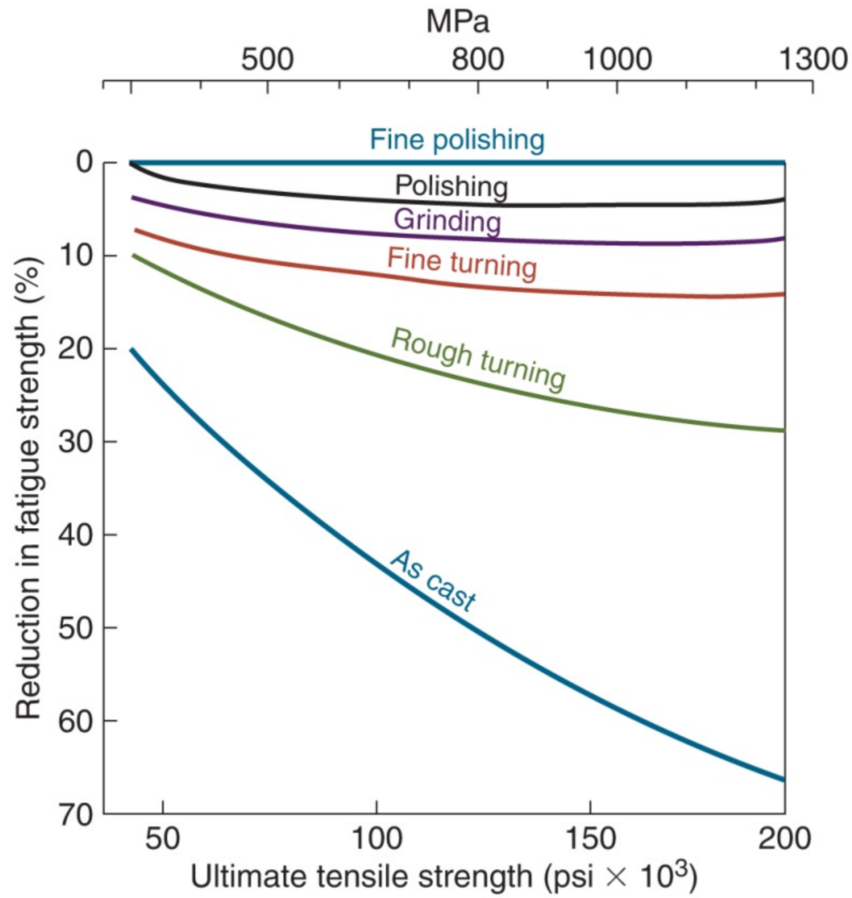

Source: M.R. Mitchell.

Figure 2.30

Residual stresses developed in bending a beam having a rectangular cross section. Note that the horizontal forces and moments caused by residual stresses in the beam must be balanced internally. Because of nonuniform deformation, especially during cold-metal working operations, most parts develop residual stresses.

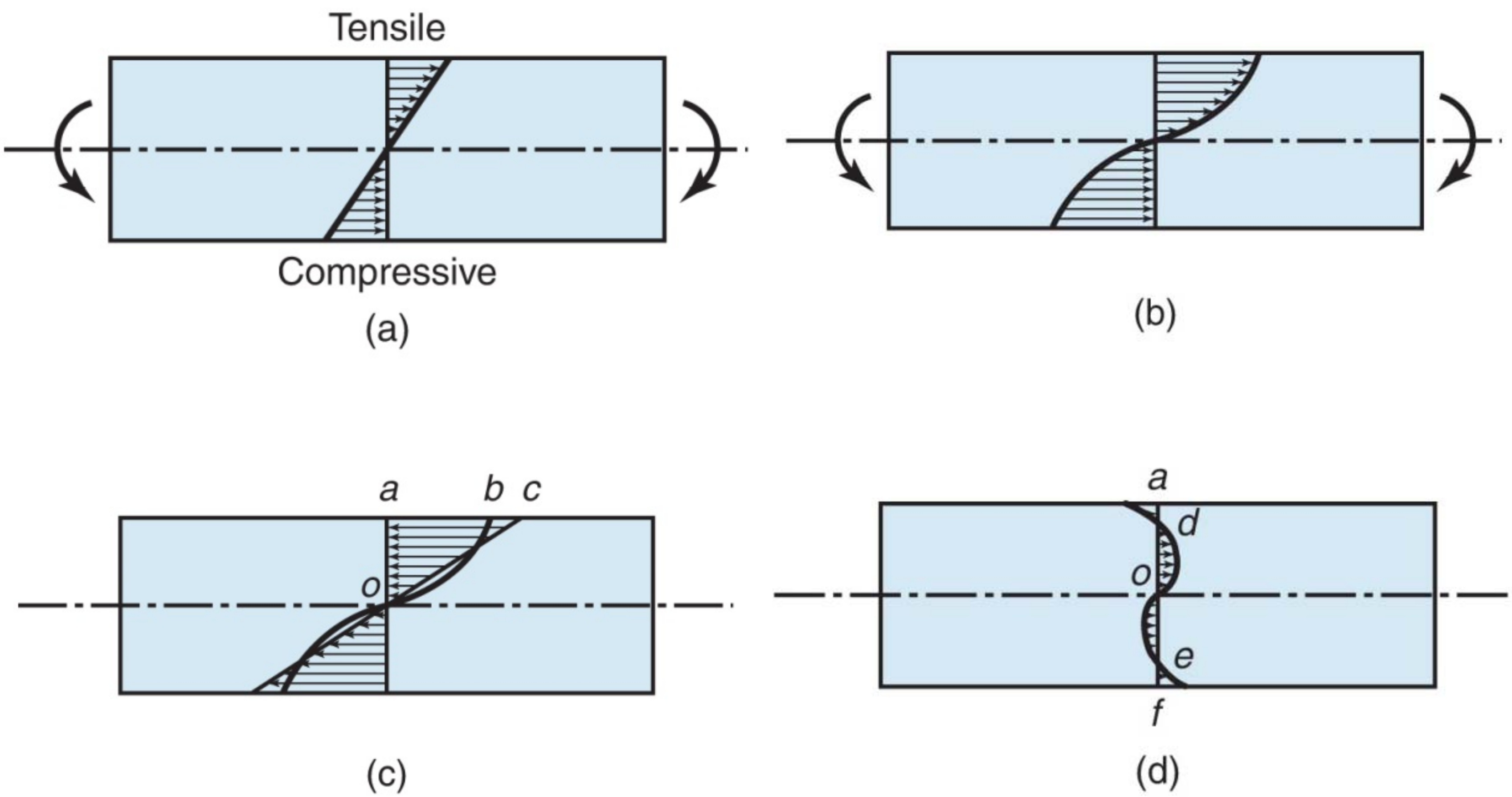

Figure 2.31

Distortion of parts with residual stresses after cutting or slitting: (a) flat sheet or plate; (b) solid round rod; (c) thin-walled tubing or pipe.